This article has been accepted for publication in a future issue of this journal, but has not been fully edited. Content may change prior to final publication. Citation information: DOI10.1109/tvt.2023.3265963, IEEE Transactions on Vehicular Technology

Energy Optimization for IRS-Aided SWIPT under Imperfect Cascaded Channels

Chiya Zhang, *Member, IEEE,* Yin Huang, Chunlong He, *Member, IEEE,* Cunhua Pan, *Member, IEEE,* Kezhi Wang, *Member, IEEE*

***Abstract*—In this paper, intelligent reflecting surface is deployed in simultaneous wireless information and power transfer (SWIPT) system to improve the energy harvesting performance. We investigate the robust beamforming design considering the impact of the imperfect cascaded channels. We maximize the minimum received energy among all energy receivers to ensure fairness, while guaranteeing the worst-case information receivers rate requirement. To address with the coupling effect of multiple variables in the optimization problem, the alternate optimization method is utilized to decouple the optimization problem into two sub-problems, and the successive convex approximation and the semidefinite relaxation methods are used to solve the sub-problems. Simulation results reveal that employing IRS into SWIPT system can enhance the energy harvest performance, Additionally, our proposed two algorithms converges rapidly and can guarantee the robustness of the system.**

***Index Terms*—Intelligent reflecting surface, simultaneous wireless information and power transfer, max-min energy.**

I. Introduction

It is believed that the next generation wireless communication will support massive Internet of Things (IoT) device with restricted energy storage capability. To support the above vision, energy harvesting technologies utilizing solar and wind energy have been proposed to enable possible self-sustainability of power-constrained communication devices. However, these technologies are vulnerable to environmental changes. Radio frequency (RF) energy harvesting has been emerged as a promising supplement, as it can enable simultaneous wireless information and power transfer (SWIPT) [1]. In [1], a multiuser multiple-input single-output (MISO) SWIPT system was studied, where weighted sum-power was maximized, while guaranteeing the minimum signal-to-interference-plus-noise ratio (SINR) requirements at the information receivers (IRs). In [2], the authors revealed that there exists a tradeoff between information rate attained and the amount of harvested energy in massive multiple-input–multiple-output (MIMO) SWIPT systems for maximizing the efficiency. The efficiencies of SWIPT depends on the signal attenuation, and the transmit power of IoT devices is typically in the order of mW. However, the harvested energy from the SWIPT technology typically ranges from 1μW to tens of μW [3]. In order to implement SWIPT, the researchers in [4] proposed a scheme of Unmanned aerial vehicle enabled SWIPT, where a UAV acts as a wireless charger to deliver energy to energy receiver. Moreover, various techniques such as massive MIMO [2], [5], [6], high-order modulation, etc., have been proposed to facilitate the energy efficiency, whereas they usually led to high capital expense [7].

Recently, intelligent reflecting surface (IRS) has been proposed as a promising technology to reconstruct the wireless channel propagation environment and enhance the performance of wireless communication systems [8]. IRS is composed of many reflective elements, and each reflective element can be programmed to change its phase. Thus, the signals reflected from the IRS can be coherently superimposed at the receiver to enhance the desired signal power, or coherently canceled to suppress the interference signal. The reflecting elements of IRS are passive and only reflect signals without amplifying them. It can be implemented with low hardware and energy cost. Furthermore, IRS can be fabricated very thin for easy deployment on walls and glass. Deploying IRS may not change the existing network architecture. In [9], in order to minimize the transmit power at the BS, the semi-definite relaxation (SDR) and alternating optimization (AO) methods were first proposed to jointly optimize the active beamforming vectors at the base station (BS) and the passive phase shift matrix of IRS, and the power scaling law of IRS aided wireless communication was also analyzed, which demonstrated that IRS can significantly improve communication system performance. In [10], the author explored the potential of IRS assisted MIMO communication system. In [11], the author maximized the energy efficiency of IRS-assisted wireless communication system. Simulation results showed that IRS can enhance system energy efficiency significantly. Extensive efforts have been devoted to IRS-aided various wireless communication systems. In [12], IRS was introduced in device-to-device communications system, and block coordinate descent (BCD) method was adopted to maximize the throughput. IRS

This work was supported in part by the National Natural Science Foundation of China under Grant 62101161, in part by Shenzhen Basic Research Program under Grant 20200811192821001, JCYJ20190808122409660, and Grant JCYJ20220531103008018, in part by Guangdong Basic Research Program under Grant 2019A1515110358, Grant 2021A1515012097, Grant 2020ZDZX1037, Grant 2020ZDZX1021, in part by the open research fund of National Mobile Communications Research Laboratory, Southeast University under Grant 2022D02.

C. Zhang is with the School of Electronic and Information Engineering, Harbin Institute of Technology, Shenzhen 518055, China, and also with the Peng Cheng Laboratory (PCL), Shenzhen 5180523, China, and also with the National Mobile Communications Research Laboratory, Southeast University, Nanjing 211189, China.(e-mail:chiya.zhang@foxmail.com).

Y. Huang and C. He are with the Guangdong Key Laboratory of Intelligent Information Processing, Shenzhen University, Shenzhen 518060, China.

C. Pan is with the National Mobile Communications Research Laboratory, Southeast University, Nanjing 210096, China.

Kezhi Wang is with Department of Computer Science, Brunel University London, Uxbridge, Middlesex, UK, UB8 3PH (email: kezhi.wang@brunel.ac.uk).

The corresponding authors are Y. Huang and C. He (email:2070436066@email.szu.edu.cn, hclong@szu.edu.cn).

This article has been accepted for publication in a future issue of this journal, but has not been fully edited. Content may change prior to final publication. Citation information: DOI10.1109/tvt.2023.3265963, IEEE Transactions on Vehicular Technology

was also adopted in multi-cells to improve cell-edge users' rate [13]. Mobile edge computing (MEC) can be used to compute offload services, [14] proposed a collaborative method based on MEC and cloud computing to offload the service to the vehicles in the vehicle network, IRS can be deployed in MEC systems to reduce the systems latency [15]. IRS also can be implemented improve physical layer security [16]–[19].

Motivated by the success of IRS-aided wireless communication systems, we aim to deploy an IRS in SWIPT system to help compensate the severe RF signal attenuation and enhance the harvested power of energy receivers (ERs). In [20], an IRS was deployed into MIMO SWIPT system to enhance the energy harvest power. In order to maximize the weighted sum rate, a BCD algorithm was used to jointly optimize the transmit precoding (TPC) matrices of the BS and phase shift matrix of the IRS. In [21], an IRS was introduced into the MISO SWIPT system, and the transmit power at access point (AP) was minimized subject to the SINR constraints at information receivers (IRs) and energy harvesting constraints at energy receivers (ERs). Instead of using exist alternating optimization (AO) approach, a penalty-based algorithm with better performance was proposed. The authors in [22] introduced an novel energy efficiency indicator and maximized the energy efficiency in an IRS-aided MISO SWIPT system. Moreover, a manifold method was used to handle the unit-modulus constraints of IRS. The weighted sum power maximization problem was investigated in an IRS-aided SWIPT system, and the authors proved that dedicated energy beam not be needed to serve both ERs and IRs [23], while the minimum received energy problem consider fairness was studied in [24]. The intelligent omni-surfaces (IOSs) allows simultaneous signal reflection and refraction, can achieve full-dimensional wireless communications for coverage extension. The introduction of IOS in SWIPT system can achieve power splitting, thus achieving more flexible scheduling of these IoT devices [25]. In addition to the passive IRS, the active IRS [26], which can adjust signal amplitude and phase has received widespread attention. In [27], an active IRS-aided SWIPT system was studied, the results demonstrated that using the active IRS can achieve more significant performance gains than using passive IRS. The authors of [28] studied the throughput maximization problem for an active IRS-aided wireless powered communication system, it was shown that the active IRS should be deployed close to the receiver, which different form the passive IRS that should be deployed near either the transmitter or receiver. In [29], an active or passive IRS was used to assist communication. The simulation results demonstrated that when the number of reflecting elements is sufficiently large or the active-IRS amplification power is too small, the passive IRS has higher achievable rates than the active IRS.

All the researches mentioned above assumed the BS knowing the accurate channel statement information (CSI). However, the IRS is passive and does not contain RF chains, so it may not send pilot signal to assist channel estimation. This will cause inevitably channel estimation errors, which can induce serious system performance loss. Hence, the robust beamforming design is crucial in the IRS-aided communication system. In [30], the authors considered the CSI of IRS to users is uncertain, and worst case robust beamforming design problem was proposed. SCA, penalty convex-concave procedure (CCP) and AO methods were adopted to solve this optimization problem. Different form [30], the author in [31] considered a more practical case of imperfect cascaded channel. Moreover, S-procedure, Bernstein-type inequality were used to handle the non-convex constraints. In [32], perfect and imperfect CSI case were considered, and different from [30], which used an approximations for worst case rate constraints, the authors proposed an equivalent transformation form of worst case rate constraints.

To the best of our knowledge, there is a paucity of IRS-assisted SWIPT system with imperfect CSI contributions in the literature. [33] studied an IRS-aided MISO SWIPT system where receivers applied power-splitting (PS) and a nonlinear energy harvesting model was used. Specifically, the authors minimized total BS transmit by jointly optimizing the beamforming weights of the BS, phase shifts of the IRS and the PS ratios of receivers. Moreover, the perfect and imperfect CSI was considered. Reference [34] investigated the robust beamforming design in an IRS-aided secrecy MISO SWIPT network. Specifically, the authors considered that the ERs were potential eavesdroppers and imperfect CSI of the direct and cascaded channels could be obtained. To ensure fairness, the transmit precoding (TPC) matrices of the BS and phase shift matrix of the IRS were jointly optimized to maximize the minimum robust information rate among the IRs. In addition, bounded and probabilistic CSI error models were considered, and AO, SCA methods were used to solve the formulated optimization problem. In this paper, we study the IRS-aided SWIPT MISO system with imperfect CSI. Since the lifetime of a self-sustainment IoT system depends on the working time of the network node, maximizing the minimum received energy among all energy receivers (ERs) is important [35]. We aim to maximize the minimum received energy among all ERs subject to minimum SINR constraint at each information receiver. Our main contributions can be summarized as follows:

1) We aim to maximize the minimum received energy among all ERs by jointly designing the active and passive beamforming vectors under the worst-case SINR constraints. To the best of our knowledge, this is the first work to study the maximization of the minimum received energy in IRS-aided SWIPT systems with imperfect cascaded channel. [20]–[24] studied IRS-aided SWIPT systems, but didn't considered imperfect CSI. [33] considered the imperfect CSI, but it assumed IRS-user channels were imperfect. In contrast, we consider a more practical case that cascaded BS-IRS-user channels are imperfect. Additionally, [33], [34] have considered different optimization problems, which are maximizing the minimum rate at the IR and minimizing the transmit power at BS, respectively. Thus, our formulated optimization problem is novel and has not been considered before. Different from the robust design under the outage probability constraints [36], the worst-case robust design we proposed can ensure the achievable rate of each user is not lower than minimum rate requirement under all possible channel errors. Moreover, the formulated optimization problem much more challenging than

This article has been accepted for publication in a future issue of this journal, but has not been fully edited. Content may change prior to final publication. Citation information: DOI10.1109/tvt.2023.3265963, IEEE Transactions on Vehicular Technology

the transmit power minimization problem in [33] since the latter can be readily transformed into a convex optimization problem.

2) The formulated optimization problem is challenging to solve, since the objective function is very complex and the optimization variables are highly coupled. Additionally, because of the uncertainty of CSI, the SINR constraints equivalent to infinitely non-convex inequality constraints. Moreover, the existing robust beamforming algorithms developed in [30] and [33] are not applicable when the imperfect cascaded channel is considered. To address this optimization problem, firstly, S-procedure is used to approximate the infinitely inequality constraints. Then, an AO method is adopted for alternately optimizing the active and passive beamforming vectors, until convergence is achieved. Specially, the SCA-based AO algorithm and SDR-based AO algorithms are proposed to solve the optimization problem. Moreover, an algorithm for selecting feasible initial points is proposed for the proposed SCA-based AO algorithm efficiently.

3) Simulation results reveal that deploy IRS in SWIPT system can enhance the energy harvest performance of ERs. Furthermore, the simulation results verify that our proposed two algorithms converge rapidly, and the robustness of the proposed algorithms are demonstrated.

The remainder of this paper is organized as follows. We introduce the system model and gives the problem formulation in Section II. Two robust beamforming design algorithms are proposed to solve the optimization problem in Section III. Section IV presents the simulation results and discussions. Finally, concluding remarks are provided in Section V.

Notations: In this paper, diag($\mathbf{x}$) returns a square diagonal matrix with each main diagonal elements being corresponding the element of vector $\mathbf{x}$. $\|\mathbf{x}\|$ denotes the ℓ_2-norm of vector $\mathbf{x}$, arg($\mathbf{x}$) means the phase extraction form the $\mathbf{x}$. $[\mathbf{x}]_{(1:N)}$ denotes the vector that contains the first N elements in $\mathbf{x}$. $\mathcal{CN}(\mathbf{x}, \mathbf{\Sigma})$ represents random vector with mean vector $\mathbf{x}$ and covariance matrix $\mathbf{\Sigma}$.Re$\{\cdot\}$ denotes the real part. $\mathbb{E}(\cdot)$ denotes the expectation operation. For matrices $\mathbf{A}$ and $\mathbf{B}$, the kronecker product between $\mathbf{A}$ and $\mathbf{B}$ is denoted by $\mathbf{A} \otimes \mathbf{B}$, the positive semi-definite of $\mathbf{A} - \mathbf{B}$ is denoted $\mathbf{A} \succeq \mathbf{B}$. The symbols $\mathbf{A}^*$, $\mathbf{A}^T$, $\mathbf{A}^H$, $\|\mathbf{A}\|_F$, Rank($\mathbf{A}$), Tr($\mathbf{A}$) and $\mathbf{A}(i,j)$ denote the conjugate, transpose, Hermitian, Frobenius norm, rank, trace and (i,j)th entry of matrix $\mathbf{A}$, respectively.

II. System Model and Problem Formulation

A. Signal Transmission Model

As shown in Fig. 1, we consider an IRS-assisted multiuser MISO SWIPT system composed of a BS with $N > 1$ antennas, an IRS with M reflecting elements, K_I single antenna IRs and K_E single antenna ERs. We denote $\mathcal{K}_I$ and $\mathcal{K}_E$ as the sets of IRs and ERs, respectively. $\boldsymbol{h}_{d,i}^H \in \mathbb{C}^{1\times N}$ and $\boldsymbol{h}_{r,i}^H \in \mathbb{C}^{1\times M}$ denote the equivalent channels from the BS to the i-th IR and the IRS to the i-th IR, respectively. $\boldsymbol{g}_{d,j}^H \in \mathbb{C}^{1\times N}$ and $\boldsymbol{g}_{r,j}^H \in \mathbb{C}^{1\times M}$ denote the counterpart channels for the j-th ER. $\boldsymbol{F} \in \mathbb{C}^{M\times N}$ denote the channel matrix from the BS to the IRS. We denote the phase shift matrix of IRS by $\mathbf{\Theta}$ = diag$\{e^{j\theta_1}, ..., e^{j\theta_m}, ..., e^{j\theta_M}\}$. Here $\theta_m \in [0, 2\pi]$ indicates the phase shift of the m-th reflecting element. Meanwhile, we assume that the BS transmits energy and information beam to each ER and IR, respectively, in order to consider the influence of energy beam on ERs energy harvesting performance. Thus, the signal transmitted by the BS can be expressed as

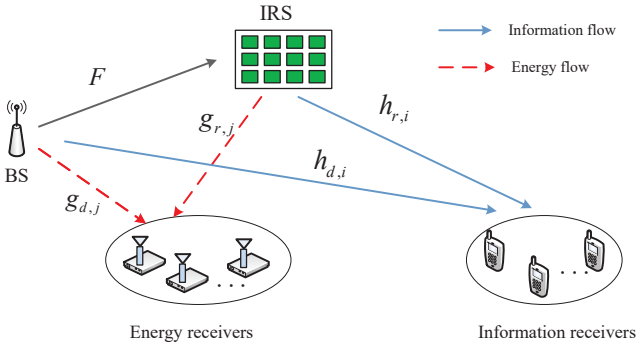

Fig. 1. System Model.

$$\boldsymbol{x} = \sum_{i\in\mathcal{K}_I} \boldsymbol{w}_i s_i^I + \sum_{j\in\mathcal{K}_E} \boldsymbol{v}_j s_j^E, \tag{1}$$

where $\boldsymbol{w}_i \in \mathbb{C}^{N\times 1}$ and $\boldsymbol{v}_j \in \mathbb{C}^{N\times 1}$ are the beamforming weights for the i-th IR and the j-th ER, while s_i^I and s_j^E denote the data symbol designated for IR and ER, respectively. It is assumed that s_i^I are independent random variables satisfying $s_i^I \sim \mathcal{CN}(0,1), \forall i \in \mathcal{K}_I$. In addition, since energy-carrying signals s_j^E,s has no useful information, they can be designed as independent random signals satisfying $\mathbb{E}(|s_j^E|^2) = 1, \forall j \in \mathcal{K}_E$. The transmit power at the BS is expressed as

$$\mathbb{E}(\boldsymbol{x}^H\boldsymbol{x}) = \sum_{i\in\mathcal{K}_I} \|\boldsymbol{w}_i\|^2 + \sum_{j\in\mathcal{K}_E} \|\boldsymbol{v}_j\|^2. \tag{2}$$

The received baseband signal can be expressed as

$$y_i^I = (\boldsymbol{h}_{r,i}^H \mathbf{\Theta} \boldsymbol{F} + \boldsymbol{h}_{d,i}^H)\boldsymbol{x} + n_i, i \in \mathcal{K}_I, \tag{3}$$

where $n_i \sim \mathcal{CN}(0, \sigma_i^2)$ represents the received complex Gaussian noise at the i-th IR.

Since s_j^E is generated as pseudo-random signals whose waveforms can be assumed to be known at both the BS and the IR before data transmission. We assume that each IR can perfectly cancel the interference from energy signals prior to decoding the desired signal s_i^I, which is similar to the assumption in [1]. Let us define $\boldsymbol{H}_i = diag(\boldsymbol{h}_{r,i}^H)\boldsymbol{F}$ as the cascaded channel from the BS to IR i via the IRS. The received SINR at the i-th IR is

$$SINR_i = \frac{|(\boldsymbol{h}_{d,i}^H + \boldsymbol{e}^H\boldsymbol{H}_i)\boldsymbol{w}_i|^2}{\|(\boldsymbol{h}_{d,i}^H + \boldsymbol{e}^H\boldsymbol{H}_i)\boldsymbol{W}_{-i}\|_2^2 + \sigma_i^2}, \tag{4}$$

where $\boldsymbol{W}_{-i} = [\boldsymbol{w}_1, ..., \boldsymbol{w}_{i-1}, \boldsymbol{w}_{i+1}, ..., \boldsymbol{w}_{K_I}]$, and $\boldsymbol{e} = [e_1, ..., e_M]^T \in \mathbb{C}^{M\times 1}$ denotes the vector that contains the diagonal elements of IRS phase shift matrix $\mathbf{\Theta}$.

On the other hand, each ER can harvest RF power from both information and energy signals. By ignoring the noise power, the received RF power at the j-th ER is given by

$$Q_j = \sum_{i\in\mathcal{K}_I} |\boldsymbol{g}_j^H\boldsymbol{w}_i|^2 + \sum_{k\in\mathcal{K}_E} |\boldsymbol{g}_j^H\boldsymbol{v}_k|^2, j \in \mathcal{K}_E, \tag{5}$$

This article has been accepted for publication in a future issue of this journal, but has not been fully edited. Content may change prior to final publication. Citation information: DOI10.1109/tvt.2023.3265963, IEEE Transactions on Vehicular Technology

where $\boldsymbol{g}_j^H = \boldsymbol{g}_{d,j}^H + \boldsymbol{e}^H \boldsymbol{G}_j$, $\boldsymbol{G}_j = diag(\boldsymbol{g}_{r,j}^H)\boldsymbol{F}$ denotes the cascaded channels from the BS to ER j via the IRS.

B. Channel Uncertainty Models

There are two channels in IRS-aided communication system, one is the direct channel from the BS to the user, and the other is the IRS reflection channel, which including BS to IRS channel and IRS to user channel. The direct channel can be accurately estimated by the traditional methods. However, the IRS reflection channel is challenging to estimate because of the passive nature of IRS. In addition, we observe the cascaded BS-IRS-user channels are sufficient for system performance improvement [37], [9], and there are many existing research studying the cascaded channel estimation, i.e., [38], [39]. Additionally, the accuracy of the CSI has a great impact on IRS-aided communication system performance. In order to account for the CSI estimation error, we assume the cascaded BS-IRS-user channels are imperfect, and a bounded CSI error model is adopted to formulate the channel estimation error [30], [40]. Specifically, the CSI of the cascaded BS-IRS-user channels can be modeled as

$$\boldsymbol{H}_i = \bar{\boldsymbol{H}}_i + \Delta\boldsymbol{H}_i, \tag{6}$$

$$\Omega_{\boldsymbol{H}_i} \triangleq \{\Delta\boldsymbol{H}_i \in \mathbb{C}^{M\times N} : \|\Delta\boldsymbol{H}_i\|_F \le \epsilon_{\boldsymbol{H}_i}\}, i \in \mathcal{K}_I \tag{7}$$

$$\boldsymbol{G}_j = \bar{\boldsymbol{G}}_j + \Delta\boldsymbol{G}_j, \tag{8}$$

$$\Omega_{\boldsymbol{G}_j} \triangleq \{\Delta\boldsymbol{G}_j \in \mathbb{C}^{M\times N} : \|\Delta\boldsymbol{G}_j\|_F \le \epsilon_{\boldsymbol{G}_j}\}, j \in \mathcal{K}_E \tag{9}$$

where $\bar{\boldsymbol{H}}_i$ and $\bar{\boldsymbol{G}}_j$ are estimated CSIs for the cascaded channel of the i-th IR and the j-th ER, respectively. $\Delta\boldsymbol{H}_i$ and $\Delta\boldsymbol{G}_j$ denote the corresponding CSI estimation errors, where $\epsilon_{\boldsymbol{H}_i}$ and $\epsilon_{\boldsymbol{G}_j}$ are the radii of the bounded regions of CSI errors, which are known at the BS. This bounded CSI error model can characterize the noisy channel estimation, limited feedback, and quantization errors of the phase shifts at the IRS [32].

C. Problem Formulation

In this subsection, we consider the worst-case robust beforming optimization problem formed by the bounded CSI error model. In order to balance the performance tradeoff between IRs and ERs and guarantee the fairness among all ERs, our goal is to maximize the minimum received power among all ERs while satisfying the worst-case quality-of-service (QoS) constraints of the IR. The problem can be formulated as follows

$$(\mathrm{P1}): \max_{\{\boldsymbol{w}_i\},\{\boldsymbol{v}_j\},\boldsymbol{e}} \min_{j\in\mathcal{K}_E} Q_j \tag{10a}$$

$$\text{s.t.} \quad \min_{\Delta\boldsymbol{H}_i\in\Omega_{\boldsymbol{H}_i}} SINR_i \ge \gamma_i, i \in \mathcal{K}_I, \tag{10b}$$

$$\sum_{i\in\mathcal{K}_I} \|\boldsymbol{w}_i\|^2 + \sum_{j\in\mathcal{K}_E} \|\boldsymbol{v}_j\|^2 \le P_t, \tag{10c}$$

$$|e_m|^2 = 1, \forall m = 1,..,M, \tag{10d}$$

where γ_i is the minimum SINR requirements of the i-th IR, and P_t denotes the maximum transmission power at the BS. Note that Problem (P1) is non-convex because of the coupled variables of $\boldsymbol{w}_i$, $\boldsymbol{v}_j$ and $\boldsymbol{e}$. In particular, the SINR constraint (10b) contains infinite non-convex inequality constraints due to the continuity of the CSI uncertainty. Therefore, (P1) is challenging to be solved.

III. Algorithm Design For IRS-Assisted SWIPT Systems With Imperfect CSI

First, we introduce an auxiliary variable u to deal with the complex objective function, and (P1) can be rewritten as follows

$$(\mathrm{P2}): \max_{\{\boldsymbol{w}_i\},\{\boldsymbol{v}_j\},\boldsymbol{e},u} u \tag{11a}$$

$$\text{s.t.} \quad \min_{\Delta\boldsymbol{G}_j\in\Omega_{\boldsymbol{G}_j}} Q_j \ge u, \forall j \in \mathcal{K}_E, \tag{11b}$$

$$\min_{\Delta\boldsymbol{H}_i\in\Omega_{\boldsymbol{H}_i}} SINR_i \ge \gamma_i, i \in \mathcal{K}_I, \tag{11c}$$

$$\sum_{i\in\mathcal{K}_I} \|\boldsymbol{w}_i\|^2 + \sum_{j\in\mathcal{K}_E} \|\boldsymbol{v}_j\|^2 \le P_t, \tag{11d}$$

$$|e_m|^2 = 1, \forall m = 1,..,M. \tag{11e}$$

Then, two efficient algorithms are proposed to solve (P2). One is SCA-based alternate optimization algorithm, and the other is the SDR-based alternate optimization algorithm.

A. Proposed SCA-Based Alternate Optimization Algorithm

In (P2), constraint (11b) is addressed by approximating the non-convex parts and then use the S-Procedure to deal with the infinite inequalities. Specifically, the following lemma can be used to linear approximation of the harvest power in (11b).

Lemma 1. *Substituting $\boldsymbol{G}_j = \bar{\boldsymbol{G}}_j + \Delta\boldsymbol{G}_j$ into the harvest power in (11b) and denote $\boldsymbol{w}_i^{(n)}$, $\boldsymbol{v}_j^{(n)}$ and $\boldsymbol{e}^{(n)}$ as the optimal solutions obtained at iteration n, then $\sum_{i\in\mathcal{K}_I}|\boldsymbol{g}_j^H\boldsymbol{w}_i|^2 + \sum_{k\in\mathcal{K}_E}|\boldsymbol{g}_j^H\boldsymbol{v}_k|^2$ is linearly approximated by its lower bound at $(\boldsymbol{w}_1^{(n)},..,\boldsymbol{w}_{K_I}^{(n)},\boldsymbol{v}_1^{(n)},..,\boldsymbol{v}_{K_E}^{(n)},\boldsymbol{e}^{(n)})$ as follows*

$$\mathrm{vec}^{\mathrm{T}}(\Delta\mathbf{G}_j)\mathbf{A}_j\,\mathrm{vec}(\Delta\mathbf{G}_j^*) + 2\,\mathrm{Re}\{\mathbf{a}_j^{\mathrm{T}}\,\mathrm{vec}(\Delta\mathbf{G}_j^*)\} + a_j, \tag{12}$$

where

$$\begin{aligned}
\mathbf{A}_j =& \boldsymbol{c}\otimes\boldsymbol{e}^*\boldsymbol{e}^{(n),T} + \boldsymbol{c}^H\otimes\boldsymbol{e}^{(n),*}\boldsymbol{e}^T - \boldsymbol{c}^{(n)}\otimes\boldsymbol{e}^{(n),*}\boldsymbol{e}^{(n),T},\\
\mathbf{a}_j =& \,\mathrm{vec}(\boldsymbol{e}(\boldsymbol{g}_{d,j}^H + \boldsymbol{e}^{(n),H}\bar{\boldsymbol{G}}_j)\boldsymbol{c}^H)\\
&+ \mathrm{vec}(\boldsymbol{e}^{(n)}(\boldsymbol{g}_{d,j}^H + \boldsymbol{e}^H\bar{\boldsymbol{G}}_j)\boldsymbol{c})\\
&- \mathrm{vec}(\boldsymbol{e}^{(n)}(\boldsymbol{g}_{d,j}^H + \boldsymbol{e}^{(n),H}\bar{\boldsymbol{G}}_j)\boldsymbol{c}^{(n)}),\\
a_j =& 2\,\mathrm{Re}\{(\boldsymbol{g}_{d,j}^H + \boldsymbol{e}^{(n),H}\bar{\boldsymbol{G}}_j)\boldsymbol{c}^H(\boldsymbol{g}_{d,j} + \bar{\boldsymbol{G}}_j^H\boldsymbol{e})\}\\
&- (\boldsymbol{g}_{d,j}^H + \boldsymbol{e}^{(n),H}\bar{\boldsymbol{G}}_j)\boldsymbol{c}^{(n)}(\boldsymbol{g}_{d,j} + \bar{\boldsymbol{G}}_j^H\boldsymbol{e}^{(n)}),\\
\boldsymbol{c} =& \sum_{i\in\mathcal{K}_I}\boldsymbol{w}_i\boldsymbol{w}_i^{(n),H} + \sum_{j\in\mathcal{K}_E}\boldsymbol{v}_j\boldsymbol{v}_j^{(n),H}.
\end{aligned}$$

Proof: See Appendix A. ■

By linear approximation the harvest power Q_j in (11b) with (12), constraint (11b) can be reformulated as

$$\begin{aligned}
&\mathrm{vec}^{\mathrm{T}}(\Delta\mathbf{G}_j)\mathbf{A}_j\,\mathrm{vec}(\Delta\mathbf{G}_j^*) + 2\,\mathrm{Re}\{\mathbf{a}_j^{\mathrm{T}}\,\mathrm{vec}(\Delta\mathbf{G}_j^*)\}\\
&+ a_j \ge u, \forall j \in \mathcal{K}_E.
\end{aligned} \tag{13}$$

Constraint (13) still contains infinite inequality constraints due to the channel uncertainty $\Delta\mathbf{G}_j$. To address this difficulty, we use the following lemma to tackle the CSI uncertainty.

This article has been accepted for publication in a future issue of this journal, but has not been fully edited. Content may change prior to final publication. Citation information: DOI10.1109/tvt.2023.3265963, IEEE Transactions on Vehicular Technology

Lemma 2. *(S-Procedure [41]) Let $g_i, i \in \{1,2\}$ be a real-valued function of vector $\boldsymbol{x}$ that is given by*

$$g_i(\boldsymbol{x}) = \boldsymbol{x}^H \boldsymbol{A}_i \boldsymbol{x} + 2\Re(\mathbf{a}_i^H \boldsymbol{x}) + a_i,$$

where $a_i \in \mathcal{R}$. Then, $g_1(\boldsymbol{x}) \leq 0 \Rightarrow g_2(\boldsymbol{x}) \leq 0$ holds if and only if there exists a variable $w \geq 0$ such that

$$w \begin{bmatrix} \mathbf{A}_1 & \mathbf{a}_1 \\ \mathbf{a}_1^H & a_1 \end{bmatrix} - \begin{bmatrix} \mathbf{A}_2 & \mathbf{a}_2 \\ \mathbf{a}_2^H & a_2 \end{bmatrix} \succeq \mathbf{0}.$$

Then, constraint (13) can be rewritten by applying Lemma 2 as follows

$$\begin{bmatrix} q_j \mathbf{I}_{MN} + \mathbf{A}_j & \mathbf{a}_j \\ \mathbf{a}_j^T & a_j - u - q_j \epsilon_{G_j}^2 \end{bmatrix} \succeq \mathbf{0}, \forall j \in \mathcal{K}_E, \quad (14)$$

where $q_j \geq 0$ are slack variables.

Next, by defining an auxiliary variable $\beta_i = \|(\boldsymbol{h}_{d,i}^H + \boldsymbol{e}^H \boldsymbol{H}_i)\boldsymbol{W}_{-i}\|_2^2 + \sigma_i^2$. Then constraints (11c) are rewritten as

$$|(\boldsymbol{h}_{d,i}^H + \boldsymbol{e}^H \boldsymbol{H}_i)\boldsymbol{w}_i|^2 \geq \beta_i \gamma_i, \forall i \in \mathcal{K}_I, \quad (15)$$

$$\|(\boldsymbol{h}_{d,i}^H + \boldsymbol{e}^H \boldsymbol{H}_i)\boldsymbol{W}_{-i}\|_2^2 + \sigma_i^2 \geq \beta_i, \forall i \in \mathcal{K}_I. \quad (16)$$

Specifically, we notice that (15) is similar to (11b). By replacing the channel associated with the ER by the channel associated with the IR (i.e., $\boldsymbol{g}_{d,j} = \boldsymbol{h}_{d,j}$, $\bar{\boldsymbol{G}}_j = \bar{\boldsymbol{H}}_i$), and setting $\boldsymbol{c} = \boldsymbol{w}_i \boldsymbol{w}_i^{(n),H}$, constraint (15) can also be transformed into the equivalent LMIs constraint, as follows

$$\begin{bmatrix} \varpi_i \mathbf{I}_{MN} + \mathbf{A}_j & \mathbf{a}_j \\ \mathbf{a}_j^T & a_j - \beta_i \gamma_i - \varpi_i \epsilon_{H_i}^2 \end{bmatrix} \succeq \mathbf{0}, \forall i \in \mathcal{K}_I. \quad (17)$$

Next, we consider the uncertainty of $\{\Delta \boldsymbol{H}_i\}$ in (16), the Schur's complement Lemma [42] is used to rewrite the inequalities in (16) as follows.

$$\begin{bmatrix} \beta_i - \sigma_i^2 & \boldsymbol{d}_i^H \\ \boldsymbol{d}_i & \boldsymbol{I} \end{bmatrix} \succeq \mathbf{0}, \forall i \in \mathcal{K}_I, \quad (18)$$

where $\boldsymbol{d}_i = ((\boldsymbol{h}_{d,i}^H + \boldsymbol{e}^H \boldsymbol{H}_i)\boldsymbol{W}_{-i})^H$. Substituting $\boldsymbol{H}_i = \bar{\boldsymbol{H}}_i + \Delta \boldsymbol{H}_i$ into (18), it can be rewritten as

$$\begin{aligned} \begin{bmatrix} \beta_i - \sigma_i^2 & \widehat{\mathbf{d}}_i^H \\ \widehat{\mathbf{d}}_i & \boldsymbol{I} \end{bmatrix} \succeq & - \begin{bmatrix} \mathbf{0} \\ \boldsymbol{W}_{-i}^H \end{bmatrix} \Delta \boldsymbol{H}_i^H \begin{bmatrix} \boldsymbol{e} & \mathbf{0} \end{bmatrix} \\ & - \begin{bmatrix} \boldsymbol{e}^H \\ \mathbf{0} \end{bmatrix} \Delta \boldsymbol{H}_i \begin{bmatrix} \mathbf{0} & \boldsymbol{W}_{-i} \end{bmatrix}, \forall i \in \mathcal{K}_I, \end{aligned} \quad (19)$$

where $\widehat{\mathbf{d}}_i = ((\boldsymbol{h}_{d,i}^H + \boldsymbol{e}^H \boldsymbol{H}_i)\boldsymbol{W}_{-i})^H$. Then we convert this constraint by leveraging the following lemma [43].

Lemma 3. *(Sign-definiteness) For matrices $\mathbf{F} = \mathbf{F}^H, \mathbf{A}, \mathbf{B}$, the following inequality satisfies*

$$\mathbf{F} \succeq \mathbf{A}^{\mathrm{H}} \mathbf{X} \mathbf{B} + \mathbf{B}^{\mathrm{H}} \mathbf{X}^{\mathrm{H}} \mathbf{A}, \forall \|\mathbf{X}\|_F \leq \xi,$$

if and only if there exist $\mu \geq 0$ such that

$$\begin{bmatrix} \mathbf{F} - \mu \mathbf{B}^{\mathrm{H}} \mathbf{B} & -\xi \mathbf{A}^{\mathrm{H}} \\ -\xi \mathbf{A} & \mu \mathbf{I} \end{bmatrix} \succeq \mathbf{0}.$$

The following parameters for each constraint in (19) can be chosen to use Lemma 3

$$\mathbf{F} = \begin{bmatrix} \beta_i - \sigma_i^2 & \widehat{\mathbf{d}}_i^{\mathrm{H}} \\ \widehat{\mathbf{d}}_i & \mathbf{I} \end{bmatrix}, \mathbf{A} = - \begin{bmatrix} \mathbf{0} & \mathbf{W}_{-i} \end{bmatrix},$$
$$\mathbf{B} = \begin{bmatrix} \mathbf{e} & \mathbf{0} \end{bmatrix}, \qquad \mathbf{X} = \Delta \mathbf{H}_i^{\mathrm{H}}.$$

Next, we have the equivalent constraints of (16) as follows

$$\begin{bmatrix} \beta_i - \sigma_i^2 - \nu_i M & \widehat{\mathbf{d}}_i^{\mathrm{H}} & \mathbf{0}_{1\times N} \\ \widehat{\mathbf{d}}_i & \mathbf{I}_{(K_I-1)} & \epsilon_{H_i} \mathbf{W}_{-i}^{\mathrm{H}} \\ \mathbf{0}_{N\times 1} & \epsilon_{H_i} \mathbf{W}_{-i} & \nu_i \mathbf{I}_N \end{bmatrix} \succeq \mathbf{0}, \forall i \in \mathcal{K}_I, \quad (20)$$

where $\nu_i \geq 0$ are slack variables.

Hence, the original problem (P2) is rewritten as

$$(\mathrm{P3}): \max_{\{\boldsymbol{w}_i\},\{\boldsymbol{v}_j\},\boldsymbol{e},u,\beta,q,\varpi,\nu} u \quad (21a)$$
$$\text{s.t.} \quad (14),(17),(20),(11d),(11e), \quad (21b)$$
$$q \geq 0, \varpi \geq 0, \nu \geq 0, \quad (21c)$$

where $q = [q_1,..,q_{K_E}]$, $\varpi = [\varpi_1,..,\varpi_{K_I}]$, $\nu = [\nu_1,..,\nu_{K_I}]$, $\beta = [\beta_1,..,\beta_{K_I}]$. Due to the coupling effect of $\{\boldsymbol{w}_i\}$ and $\boldsymbol{e}$, it is difficult to optimize $\{\boldsymbol{w}_i\}$ and $\boldsymbol{e}$ simultaneously. Hence, the alternating optimization method is used to solve this problem. In particular, by fixing the phase shift vector $\boldsymbol{e}$, the optimized active beamforming vectors $\{\boldsymbol{w}_i\}$, $\{\boldsymbol{v}_j\}$ are obtained, then fixing the active beamforming vectors, the optimized phase shift vectors $\boldsymbol{e}$ are obtained. Finally, the optimal value of $\{\boldsymbol{w}_i\}$, $\{\boldsymbol{v}_j\}$ and $\boldsymbol{e}$ can be obtained through iterations. We can get the subproblem of $\{\boldsymbol{w}_i\}, \{\boldsymbol{v}_j\}$ as follows

$$(\mathrm{P4}): \max_{\{\boldsymbol{w}_i\},\{\boldsymbol{v}_j\},u,\beta,q,\varpi,\nu} u \quad (22a)$$
$$\text{s.t.} \quad (14),(17),(20),(11d),(21c). \quad (22b)$$

(P4) is an SDP problem, which can be solved by using CVX.

Then, we optimize the phase shift vectors $\boldsymbol{e}$ for given $\{\boldsymbol{w}_i\}, \{\boldsymbol{v}_j\}$. The optimization problem can be expressed as

$$(\mathrm{P5}): \max_{\boldsymbol{e},u,\beta,q,\varpi,\nu} u \quad (23a)$$
$$\text{s.t.} \quad (14),(17),(20),(11e),(21c). \quad (23b)$$

(P5) is still non-convex because of the unit-modulus constraint (11e). Next, a penalty convex-concave procedure (CCP) method is used to obtain a sub-optimal solution. Specifically, constraint $|e_m|^2 = 1, \forall m = 1,..,M$, can be equivalently transformed into $1 \leq |e_m|^2 \leq 1, \forall m = 1,..,M$. Notice that constraint $1 \leq |e_m|^2$ is non-convex, hence, we linearize it as $|e_m^{(n)}|^2 - 2\,\mathrm{Re}(e_m^* e_m^{(n)}) \leq -1, \forall m = 1,..,M$, at fixed $e_m^{(n)}$. Then, we can reformulate (P5) as follows

$$(\mathrm{P5.1}): \max_{\boldsymbol{e},u,\beta,q,\varpi,\nu} u - \frac{1}{\rho}\sum_{m=1}^{2M} \tau_m \quad (24a)$$
$$\text{s.t.} \quad (14),(17),(20),(21c),\boldsymbol{\tau} \geq 0, \quad (24b)$$
$$|e_m^{(n)}|^2 - 2\mathrm{Re}(e_m^* e_m^{(n)}) \leq -1 + \tau_{M+m}, \quad (24c)$$
$$|e_m|^2 \leq 1 + \tau_m, \forall m = 1,..,M, \quad (24d)$$

where $\boldsymbol{\tau} = [\tau_1,...,\tau_{2M}]^T$ are the slack variables, $1/\rho$ is a regularization factor to scale the penalty item $||\boldsymbol{\tau}||_1$, and it can control the feasibility of the unit-modulus constraints. Specifically, when the value of $1/\rho$ is too large, a feasible solution may not be found. However, a smaller value of $1/\rho$ may cause dissatification on unit-modulus constraints. Hence, we gradually increase the value of the penalty coefficient $1/\rho$, until satisfying predefined accuracy. (P5.1) is an SDP problem

This article has been accepted for publication in a future issue of this journal, but has not been fully edited. Content may change prior to final publication. Citation information: DOI10.1109/tvt.2023.3265963, IEEE Transactions on Vehicular Technology

and can be solved by the CVX tool. Finally, the problem (P1) can be solved iteratively by employing (P4) and (P5.1). The SCA based alternate optimization algorithm is given in Algorithm 1.

Algorithm 1 SCA-Based Alternate Optimization Algorithm

Input: Initialize $\boldsymbol{w}_i^{(0)}$, $\boldsymbol{v}_j^{(0)}$ for $\forall i \in \mathcal{K}_I, j \in \mathcal{K}_E$, and $\boldsymbol{e}^{(0)}$, set maximum number of iterations T_{max}, error tolerance ζ, $0 \leq c \leq 1$

Output: the optimal solution $\boldsymbol{w}_i^*$, $\boldsymbol{v}_j^*$, $\boldsymbol{e}^*$ and u^*.

```
Initialize: t = 0;
repeat
    Given e^(t), w_i^(t), v_j^(t), calculate w_i^(t+1), v_j^(t+1) by solving Problem (P4) ;
    Set: n = 0;
    repeat
        Given e^(t), w_i^(t), v_j^(t) and ρ^(n), calculate e^(n+1) by solving Problem (P5.1);
        ρ^(n+1) = max{cρ^(n), ρ_min};
    until ‖ τ^(n+1) ‖_1 ≤ ε_1 and ‖ e^(n+1) − e^(n) ‖_1 ≤ ε_2;
    e^(t+1) = e^(n+1);
until t ≥ T_max or (u^(t+1) − u^(t)) / u^(t+1) ≤ ζ.
return u* = u^(t+1), w_i* = w_i^(t+1), v_j* = v_j^(t+1), e* = e^(t+1).
```

Notice that it is non-trivial to initialize $\boldsymbol{w}_i^{(0)}$, $\boldsymbol{v}_j^{(0)}$, and $\boldsymbol{e}^{(0)}$. An unsuitable initial point will make the optimization problem infeasible. An algorithm is designed to find a feasible point of (P2). Considering that the optimization problem is infeasible mainly because of the fact that the minimum SINR constraint (11c) is not satisfied. Therefore, we simplified (P2) without considering the channel uncertainty and energy receivers. Specifically, we maximize the minimize SINR among all IRs, and the initial point can be guaranteed to satisfy the SINR constraint (11c). Finally, the optimal solution of the following optimization problem can be used as the initial point of Problem (P3):

$$
\begin{aligned}
(\mathrm{P6}): \max_{\{\boldsymbol{w}_i\},\boldsymbol{e},u} \quad & u && (25a)\\
\text{s.t.} \quad & |(\boldsymbol{h}_{d,i}^H + \boldsymbol{e}^H \boldsymbol{H}_i)\boldsymbol{w}_i|^2 \geq \beta_i\gamma_i + u, \forall i \in \mathcal{K}_I, && (25b)\\
& \|(\boldsymbol{h}_{d,i}^H + \boldsymbol{e}^H \boldsymbol{H}_i)\boldsymbol{W}_{-i}\|_2^2 + \sigma_i^2 \geq \beta_i, \forall i \in \mathcal{K}_I, && (25c)\\
& \sum_{i\in\mathcal{K}_I} \|\boldsymbol{w}_i\|^2 \leq P_t, && (25d)\\
& |e_m|^2 = 1. && (25e)
\end{aligned}
$$

By leveraging the Lemma 1, and set $\Delta\mathbf{G}_j = \Delta\boldsymbol{H}_i = \mathbf{0}$, $\boldsymbol{g}_{d,j} = \boldsymbol{h}_{d,j}$, $\bar{\boldsymbol{G}}_j = \bar{\boldsymbol{H}}_i$, $\boldsymbol{c} = \boldsymbol{w}_i\boldsymbol{w}_i^{(n),H}$, (25b) can be equivalently rewritten as

$$
\begin{aligned}
&2\,\mathrm{Re}\{(\boldsymbol{h}_{d,i}^H + \boldsymbol{e}^{(n),H}\boldsymbol{H}_i)\boldsymbol{w}_i^{(n)}\boldsymbol{w}_i^H(\boldsymbol{h}_{d,i} + \boldsymbol{H}_i^H\boldsymbol{e})\} -\\
&(\boldsymbol{h}_{d,i}^H + \boldsymbol{e}^{(n),H}\boldsymbol{H}_i)\boldsymbol{w}_i^{(n)}\boldsymbol{w}_i^{(n),H}(\boldsymbol{h}_{d,i} + \boldsymbol{H}_i^H\boldsymbol{e}^{(n)}) \geq \beta_i\gamma_i + u. \qquad (26)
\end{aligned}
$$

Next, the inequalities in (25c) can be equivalently converted as follows by using the Schur's complement lemma

$$
\begin{bmatrix} \beta_i - \sigma_i^2 & \boldsymbol{d}_i^H \\ \boldsymbol{d}_i & \boldsymbol{I} \end{bmatrix} \succeq \mathbf{0}, \forall i \in \mathcal{K}_I, \qquad (27)
$$

where $\boldsymbol{d}_i = ((\boldsymbol{h}_{d,i}^H + \boldsymbol{e}^H\boldsymbol{H}_i)\boldsymbol{W}_{-i})^H$. Therefore, (P6) can be reformulated as follows

$$
\begin{aligned}
(\mathrm{P6.1}): \max_{\{\boldsymbol{w}_i\},\boldsymbol{e},u} \quad & u && (28a)\\
\text{s.t.} \quad & (26), (27), (25d), (25e). && (28b)
\end{aligned}
$$

AO method can be adopted to solve the Problem (P6.1), which is similar to (P2). Denote the optimal solution of (P6.1) as $\boldsymbol{w}_i^*$ and $\boldsymbol{e}^*$, then the initial point of Algorithm 1 can be set as $\boldsymbol{w}_i^{(0)} = \boldsymbol{w}_i^*$, $\boldsymbol{e}^{(0)} = \boldsymbol{e}^*$ and $\boldsymbol{v}_i^{(0)} = \mathbf{0}$.

B. Proposed SDR-Based Alternate Optimization Algorithm

Since SCA method uses a linear approximation of the worst-case rate constraint, this may result in performance loss. We propose another novel algorithm to solve Problem (P2) by leveraging the SDR and AO technique. The numerator of the SINR in (4) is equivalently reformulated as

$$
\begin{aligned}
&|(\mathbf{h}_{d,i}^H + \mathbf{e}^H\mathbf{H}_i)\mathbf{w}_i|^2\\
&= 2\Re(\mathbf{e}^H\mathbf{H}_i\mathbf{W}_i\mathbf{h}_{d,i}) + \mathbf{e}^H\mathbf{H}_i\mathbf{W}_i\mathbf{H}_i^H\mathbf{e} + \mathbf{h}_{d,i}^H\mathbf{W}_i\mathbf{h}_{d,i} \qquad (29)\\
&= \boldsymbol{\phi}^H\mathbf{E}_i^H\mathbf{W}_i\mathbf{E}_i\boldsymbol{\phi} = \mathrm{Tr}(\boldsymbol{\Phi}\mathbf{E}_i^H\mathbf{W}_i\mathbf{E}_i),
\end{aligned}
$$

where $\mathbf{W}_i = \mathbf{w}_i\mathbf{w}_i^H$, $\mathbf{E}_i = [\mathbf{H}_i^H \quad \mathbf{h}_{d,i}]$ denote an channel matrix including both the direct channel and the IRS reflection channel, $\boldsymbol{\phi} = [\mathbf{e}^H, 1]^H$, and $\boldsymbol{\Phi} = \boldsymbol{\phi}\boldsymbol{\phi}^H$. The denominator can be equivalently reformulated in a similar manner. Hence, we can reformulate (P2) as follows

$$
\begin{aligned}
(\mathrm{P7}): \max_{\{\boldsymbol{W}_i\},\{\boldsymbol{V}_j\},\boldsymbol{\Phi},u} \quad & u && (30a)\\
\text{s.t.} \quad & \min_{\Delta\boldsymbol{G}_j\in\Omega_{\boldsymbol{G}_j}} \mathrm{Tr}(\boldsymbol{\Phi}\boldsymbol{\Xi}_j^H\mathbf{B}\boldsymbol{\Xi}_j) \geq u, \forall j \in \mathcal{K}_E, && (30b)\\
& \max_{\Delta\boldsymbol{H}_i\in\Omega_{\boldsymbol{H}_i}} \mathrm{Tr}(\boldsymbol{\Phi}\mathbf{E}_i^H\bar{\mathbf{W}}_i\mathbf{E}_i) + \gamma_i\sigma_i^2 \leq 0, \forall i \in \mathcal{K}_I, && (30c)\\
& \sum_{i\in\mathcal{K}_I} \mathrm{Tr}(\mathbf{W}_i) + \sum_{j\in\mathcal{K}_E} \mathrm{Tr}(\mathbf{V}_j) \leq P_t, && (30d)\\
& \boldsymbol{\Phi}_{mm} = 1, \forall m = 1, .., M+1, && (30e)\\
& \mathrm{Rank}(\mathbf{W}_i) = 1, \forall i \in \mathcal{K}_I, && (30f)\\
& \mathrm{Rank}(\mathbf{V}_j) = 1, \forall j \in \mathcal{K}_E, && (30g)\\
& \mathrm{Rank}(\boldsymbol{\Phi}) = 1, && (30h)
\end{aligned}
$$

where $\boldsymbol{\Xi}_j = [\mathbf{G}_j^H \quad \mathbf{g}_{d,j}]$, $\mathbf{B} = (\sum_{i\in\mathcal{K}_I}\mathbf{W}_i + \sum_{j\in\mathcal{K}_E}\mathbf{V}_j)$, $\bar{\mathbf{W}}_i = \gamma_i\sum_{k\in\mathcal{K}_I\setminus\{i\}}\mathbf{W}_k - \mathbf{W}_i$.

First, we use the S-Procedure to deal with the semi-infinite inequalities (30c). Specifically, we have

$$
\begin{aligned}
\mathbf{E}_i &= [\mathbf{H}_i^H \quad \mathbf{h}_{d,i}] = [\bar{\mathbf{H}}_i + \Delta\mathbf{H}_i \quad \mathbf{h}_{d,i}]\\
&= \bar{\mathbf{E}}_i + \Delta\mathbf{E}_i,
\end{aligned} \qquad (31)
$$

where $\bar{\mathbf{E}}_i = [\bar{\mathbf{H}}_i^H \quad \mathbf{h}_{d,i}]$ and $\Delta\mathbf{E}_i = [\Delta\mathbf{H}_i^H \quad \mathbf{0}_{N\times 1}]$. According to (6), we have

$$
\|\Delta\mathbf{E}_i\|_F = \sqrt{\|\Delta\mathbf{H}_i\|_F^2} \leq \sqrt{\epsilon_{\boldsymbol{H}_i}^2} = \epsilon_{\boldsymbol{H}_i}. \qquad (32)
$$

This article has been accepted for publication in a future issue of this journal, but has not been fully edited. Content may change prior to final publication. Citation information: DOI10.1109/tvt.2023.3265963, IEEE Transactions on Vehicular Technology

By using transformations $\mathrm{Tr}(\mathbf{A}^H\mathbf{B}\mathbf{C}\mathbf{D}) = \mathrm{vec}^H(\mathbf{A})\left(\mathbf{D}^T\otimes\mathbf{B}\right)\mathrm{vec}(\mathbf{C})$, constraint (30c) can be equivalently rewritten as follows

$$\begin{aligned}&\mathrm{Tr}(\boldsymbol{\Phi}\mathbf{E}_i^H\bar{\mathbf{W}}_i\mathbf{E}_i)+\gamma_i\sigma_i^2\\&=\mathbf{h}_i^H(\boldsymbol{\Phi}^T\otimes\bar{\mathbf{W}}_i)\mathbf{h}_i+\gamma_i\sigma_i^2\le 0,\forall\|\Delta\mathbf{E}_i\|_F\le\epsilon_{\boldsymbol{H}_i},\end{aligned}\tag{33}$$

where $\mathbf{h}_i=\mathrm{vec}(\mathbf{E}_i)$. We can define

$$\mathbf{h}_i=\bar{\mathbf{h}}_i+\Delta\mathbf{h}_i,\tag{34}$$

where $\bar{\mathbf{h}}_i=\mathrm{vec}(\bar{\mathbf{E}}_i)$, $\Delta\mathbf{h}_i=\mathrm{vec}(\Delta\mathbf{E}_i)$. Hence, $\|\Delta\mathbf{h}_i\|_2=\|\Delta\mathbf{E}_i\|_F\le\epsilon_{\boldsymbol{H}_i}$. By substituting (34) into (33), constraint (33) can be further rewritten as follows

$$\begin{aligned}&\Delta\mathbf{h}_i^H(\boldsymbol{\Phi}^T\otimes\bar{\mathbf{W}}_i)\Delta\mathbf{h}_i+\bar{\mathbf{h}}_i^H(\boldsymbol{\Phi}^T\otimes\bar{\mathbf{W}}_i)\bar{\mathbf{h}}_i\\&+2\Re(\bar{\mathbf{h}}_i^H(\boldsymbol{\Phi}^T\otimes\bar{\mathbf{W}}_i)\Delta\mathbf{h}_i)\\&+\gamma_i\sigma_i^2\le 0,\forall\|\Delta\mathbf{h}_i\|_2\le\epsilon_{\boldsymbol{H}_i}.\end{aligned}\tag{35}$$

Then, Lemma 2 can be used to deal with the channel uncertainty in constraints (35). Specifically, (35) can be rewritten as follows

$$\begin{aligned}&\mu_i\begin{bmatrix}\mathbf{I}_{N(M+1)}&\mathbf{0}\\\mathbf{0}&-\epsilon_{\boldsymbol{H}_i}^2\end{bmatrix}\\&-\begin{bmatrix}\boldsymbol{\Phi}^T\otimes\bar{\mathbf{W}}_i&(\boldsymbol{\Phi}^T\otimes\bar{\mathbf{W}}_i)\bar{\mathbf{h}}_i\\\bar{\mathbf{h}}_i^H(\boldsymbol{\Phi}^T\otimes\bar{\mathbf{W}}_i)&\bar{\mathbf{h}}_i^H(\boldsymbol{\Phi}^T\otimes\bar{\mathbf{W}}_i)\bar{\mathbf{h}}_i+\gamma_i\sigma_i^2\end{bmatrix}\succeq\mathbf{0}\\&\Leftrightarrow\mathbf{U}_i-\mathbf{P}_i^H(\boldsymbol{\Phi}^T\otimes\bar{\mathbf{W}}_i)\mathbf{P}_i\succeq\mathbf{0},\forall i\in\mathcal{K}_I,\end{aligned}\tag{36}$$

where

$$\begin{aligned}\mathbf{U}_i&=\begin{bmatrix}\mu_i\mathbf{I}_{N(M+1)}&\mathbf{0}\\\mathbf{0}&-\mu_i\epsilon_{\boldsymbol{H}_i}^2-\gamma_i\sigma_i^2\end{bmatrix},\\\mathbf{P}_i&=\begin{bmatrix}\mathbf{I}_{N(M+1)}&\bar{\mathbf{h}}_i\end{bmatrix},\end{aligned}\tag{37}$$

and $\mu=[\mu_1,...,\mu_{K_I}]^T\ge 0$ are slack variables. Hence, the infinite inequalities in (30c) are transformed into LMIs in (37), which are readily to be solved.

The constraint (30b) also contains the channel uncertainty. Firstly, constraint (30b) is rewritten as follows

$$\max_{\Delta\boldsymbol{G}_j\in\Omega_{\boldsymbol{G}_j}}\mathrm{Tr}(\boldsymbol{\Phi}\boldsymbol{\Xi}_j^H\mathbf{C}\boldsymbol{\Xi}_j)+u\le 0,\forall j\in\mathcal{K}_E,\tag{38}$$

where $\mathbf{C}=-(\sum_{i\in\mathcal{K}_I}\mathbf{W}_i+\sum_{j\in\mathcal{K}_E}\mathbf{V}_j)$. Then, we find that the above constraint (38) is similar to (30c). Hence, by using similar derivations as in (31)-(37), we have an equivalent form of (30b) as follows

$$\mathbf{X}_j-\mathbf{Z}_j^H(\boldsymbol{\Phi}^T\otimes\mathbf{C})\mathbf{Z}_j\succeq\mathbf{0},\forall j\in\mathcal{K}_E,\tag{39}$$

where

$$\begin{aligned}\mathbf{X}_j&=\begin{bmatrix}\varphi_j\mathbf{I}_{N(M+1)}&\mathbf{0}\\\mathbf{0}&-\varphi_j\epsilon_{\boldsymbol{G}_j}^2-u\end{bmatrix},\\\mathbf{Z}_j&=\begin{bmatrix}\mathbf{I}_{N(M+1)}&\bar{\mathbf{g}}_j\end{bmatrix},\end{aligned}\tag{40}$$

where $\bar{\mathbf{g}}_j=\mathrm{vec}(\bar{\boldsymbol{\Xi}}_j)$. Hence, the original robust beforming design problem (P7) can be rewritten as follows

$$(\mathrm{P8}):\max_{\{\boldsymbol{W}_i\},\{\boldsymbol{V}_j\},\boldsymbol{\Phi},u}u\tag{41a}$$

$$\mathrm{s.t.}(36),(39),(30d)-(30h).\tag{41b}$$

However, (P8) is still non-convex. Furthermore, (30f)-(30h) are rank-one constraints, which are non-convex. Next, we use the method of AO and SDR to solve this problem. Specifically, for given $\boldsymbol{\Phi}$, the subproblem of $\boldsymbol{W}_i$, $\boldsymbol{V}_j$ is given by

$$(\mathrm{P8.1}):\max_{\{\boldsymbol{W}_i\},\{\boldsymbol{V}_j\},u}u\tag{42a}$$

$$\mathrm{s.t.}(36),(39),(30d),(30f),(30g).\tag{42b}$$

The rank-one constraint (30f), (30g) can be relaxed by using SDR method. This problem becomes an SDP problem, which can be solved by convex optimization tool, i.e., CVX. We denote the optimal solution of this relaxed problem as $\boldsymbol{W}_i^*,\forall i\in\mathcal{K}_I$ and $\boldsymbol{V}_j^*,\forall j\in\mathcal{K}_E$. Then, we have the following lemma.

Lemma 4. *The optimal solution of Problem (P8.1) always satisfies the rank-one condition:* $\mathrm{rank}\,(\boldsymbol{W}_i^*)=1,\forall i\in\mathcal{K}_I,\mathrm{rank}\left(\boldsymbol{V}_j^*\right)=1,\forall j\in\mathcal{K}_E$.

Proof: See Appendix B. ■

On the other hand, we optimize the phase shift matrix $\boldsymbol{\Phi}$, when $\mathbf{W}_i,\mathbf{V}_j$ are given. The optimization problem becomes

$$(\mathrm{P8.2}):\max_{\boldsymbol{\Phi},u}u\tag{43a}$$

$$\mathrm{s.t.}(36),(39),(30e),(30h).\tag{43b}$$

By relaxing the rank-one constraint (30h), Problem (P8.2) is an SDP problem, and can be solved by CVX. We denote the optimal solution of (P8.2) as $\boldsymbol{\Phi}^*$ and u^*, if $rank(\boldsymbol{\Phi}^*)=1$, u^* is the optimal solution. Otherwise, the Gaussian randomization method can be used to construct a rank-one solution, which can find an optimal rank-one feasible solution $\boldsymbol{\Phi}$ around $\boldsymbol{\Phi}^*$. Specifically, we first perform the eigenvalue decomposition over the $\boldsymbol{\Phi}^*$ as $\boldsymbol{\Phi}^*=\mathbf{U}\boldsymbol{\Sigma}\mathbf{U}^H$. Then, we set $\boldsymbol{\phi}=\mathbf{U}\boldsymbol{\Sigma}^{\frac{1}{2}}\mathbf{r}$, where $\mathbf{r}\sim\mathcal{CN}(0,\boldsymbol{I})$ is a random $\mathbf{CSCG}$ vector. With independently generated a large number of Gaussian random vectors $\mathbf{r}$, the optimal solution $\boldsymbol{\phi}^*=e^{j\arg(\boldsymbol{\phi}/\boldsymbol{\phi}_{N+1})}$ is the one to achieve the maximum objective value of (P8.2). Finally, the IRS phase shift $\boldsymbol{\theta}$ can be recovered as $\boldsymbol{\theta}=\boldsymbol{\phi}^*_{[1:N]}$.

The SDR based AO algorithm is given in Algorithm 2.

Algorithm 2 SDR-Based Alternate Optimization Algorithm

Input: Initialize the phase shifts as $\boldsymbol{\Phi}=\boldsymbol{\Phi}^{(0)}$.
Output: the optimal solution $\boldsymbol{W}_i^*$, $\boldsymbol{V}_j^*$, $\boldsymbol{\Phi}^*$ and u^*.

1: Initialize: $t=0$;
2: **repeat**
3: Given $\boldsymbol{\Phi}^{(t)}$, calculate $\boldsymbol{W}_i^{(t+1)},\boldsymbol{V}_j^{(t+1)}$ by solving (P8.1);
4: Given $\boldsymbol{W}_i^{(t+1)},\boldsymbol{V}_j^{(t+1)}$, calculate $\boldsymbol{\Phi}^{(t+1)},u^{(t+1)}$ by solving (P8.2). If $\boldsymbol{\Phi}^{(t+1)}$ is not rank-one, The Gaussian randomization step need be used to construct a feasible rank-one solution.
5: **until** $t\ge T_{max}$ or $\frac{u^{(t+1)}-u^{(t)}}{u^{(t+1)}}\le\zeta$.
6: **return** $u^*=u^{(t+1)},\boldsymbol{W}_i^*=\boldsymbol{W}_i^{(t+1)},\boldsymbol{V}_j^*=\boldsymbol{V}_j^{(t+1)},\boldsymbol{\Phi}^*=\boldsymbol{\Phi}^{(t+1)}$.

C. Computational Complexity

In this subsection, we provide the complexity analysis of the proposed two worst-case robust beamforming design

This article has been accepted for publication in a future issue of this journal, but has not been fully edited. Content may change prior to final publication. Citation information: DOI10.1109/tvt.2023.3265963, IEEE Transactions on Vehicular Technology

algorithms. Note that all the resulting convex problems only contains LMI constraints and second-order cone (SOC) constraints. The problems are solved by the interior point method [44], and the number of iterations required to obtain the optimal solution is

$$\beta = \sqrt{\sum_{i=1}^{p} a_i + 2m}, \tag{44}$$

where p denotes the number of LMI constraints, a_i represents the dimension corresponding to the constraint, and m represents the number of SOC constraints. The complexity of each iteration is

$$C = n\sum_{i=1}^{p} a_i^3 + n^2\sum_{i=1}^{p} a_i^2 + n\sum_{i=1}^{m} k_i^2 + n^3, \tag{45}$$

where n represents the total number of variables, p and m represent the number of LMI and SOC constraints, respectively. Finally, the general expression of total complexity is $\mathcal{O}(\beta C)$. Based on this expression, the computational complexity per iteration of the proposed algorithms are given as follows

1) *SCA-Based AO algorithm*. The approximate complexity of the subproblem (P4) for optimizing the beamforming vectors is $o_{\mathbf{F}} = \mathcal{O}([(K_I+K_E)(MN+1)+K_I(K_I+N+3)+K_E+4N]^{1/2}n_1[n_1^2+n_1((K_I+K_E)(MN+1)^2+K_I(K_I+N)^2)+(K_I+K_E)(MN+1)^3+K_I(K_I+N)^3])$, where $n_1 = N(K_I+K_E)+3K_I+K_E+1$. The approximate complexity of the subproblem (P5.1) for optimizing the phase shift vectors is $o_{\mathbf{e}} = \mathcal{O}([(K_I+K_E)(MN+1)+K_I(K_I+N+3)+K_E+2M]^{1/2})n_2[n_2^2+n_2((K_I+K_E)(MN+1)^2+K_I(K_I+N)^2)+(K_I+K_E)(MN+1)^3+K_I(K_I+N)^3+M])$, where $n_2 = M+K_E+3K_I+1$. The approximate complexity of the SCA-Based AO Algorithm per iteration is $o_{\mathbf{F}} + o_{\mathbf{e}}$.
2) *SDR-Based AO algorithm*. The approximate complexity of the subproblem (P8.1) for optimizing the beamforming vectors is $o_{\mathbf{F}} = \mathcal{O}([(K_I+K_E)(MN+N+1)+1]^{1/2}n_3[n_3^2++n_3(K_I+K_E)(MN+N+1)^2+n_3+(K_I+K_E)(MN+N+1)^3+1])$, where $n_3 = (K_I+K_E)N^2+1$. The approximate complexity of the subproblem (P8.2) for optimizing the phase shift vectors is $o_{\mathbf{e}} = \mathcal{O}([(K_I+K_E)(MN+N+1)+M+1]^{1/2})n_4[n_4^2+n_4((K_I+K_E)(MN+N+1)^2+(n_4+1)(M+1)+(K_I+K_E)(MN+N+1)^3])$, where $n_4 = (M+1)^2+1$. The approximate complexity of the SCA-Based AO Algorithm per iteration is $o_{\mathbf{F}} + o_{\mathbf{e}}$.

IV. SIMULATION RESULTS

In this section, simulation setup and numerical results are provided to demonstrate the benefits of IRS-aid SWIPT system, and evaluate the performance of the proposed algorithms.

A. Simulation Setup

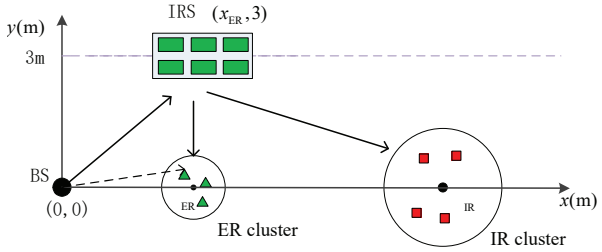

Fig. 2. Simulation setup

As seen in Fig.2, where an IRS is deployed to assist the SWIPT system. The BS is located at (0, 0) and the IRS is placed at $(x_{ER}, 3)$. The IRs and ERs are uniformly and randomly scattered in a circle centered at $(x_{IR}, 0)$ and $(x_{ER}, 0)$ with radius of 4 m and 1 m, respectively. The distance-dependent path loss model is given by

$$PL = PL_0(\frac{D}{D_0})^{-\alpha}, \tag{46}$$

where $PL_0 = (\lambda/4\pi)^2$ is the path loss at the reference distance $D_0 = 1$ m. D denotes the length of the link in meters, and α is the path loss exponent. The path loss exponents of the BS-IRS links are set to be 2.2, while the path loss exponent of BS-IRs and BS-ERs links are set to 3.6. The path loss exponents of IRS-IR and IRS-ER are set to 2.4 and 2, respectively. The small scale fading channel can be expressed as Gaussian random variables with zero mean and unit variance.

The CSI error bounds are defined as $\epsilon_{\mathrm{H}_i} = \delta_{\mathrm{h}} \left\|\mathrm{vec}\left(\bar{\mathbf{H}}_i\right)\right\|_2$ and $\epsilon_{\mathrm{G}_j} = \delta_{\mathrm{g}} \left\|\mathrm{vec}\left(\bar{\mathbf{G}}_j\right)\right\|_2$, respectively. $\delta_{\mathrm{g}} \in [0,1)$ and $\delta_{\mathrm{h}} \in [0,1)$ are the channel estimation error coefficients. Without loss of generality, we assume that the channel estimation error coefficient $\delta_{\mathrm{h}} = \delta_{\mathrm{g}} = \delta$, and all IRs have the same SINR target and noise power, i.e., $\gamma_i = \gamma_0, \sigma_i^2 = \sigma^2, \forall i \in \mathcal{K}_I$, the other parameters are set as follows: $\delta = 0.02$, $PL_0 = -30$ dB, $\sigma^2 = -80$ dBm, $N = 6$, $\gamma_0 = 1$ bit/s/Hz, $M = 40$, $P_t = 10$ W, $x_{ER} = 3$ m, $x_{IR} = 50$ m, $\mathcal{K}_I = 2$, $\mathcal{K}_E = 2$ (if not specified otherwise).

In the following, a pair of benchmark schemes are proposed to compare with our proposed algorithms: 1)'No-IRS': in this scheme, we consider the problem in the traditional SWIPT system. 2)'No Robust': the channel estimation error is ignored. 3)'Rand Phase': only the active beamforming vectors at the BS are optimized via solving the corresponding sub-problem.

B. Convergence of the Proposed Algorithms

In Fig. 3, we study the convergence behaviour of the proposed SCA-based AO algorithm and SDR-based AO algorithm for different numbers of reflecting elements at IRS M is investigated. It is observed from Fig. 3 that both the two proposed algorithms can converge in several iterations. In addition, the SDR-based AO algorithm requires much smaller number of iterations to converge than the SCA-based AO algorithm. However, both the proposed algorithms converge within 5 iterations on average, which shows the low complexity of the proposed two algorithms.

This article has been accepted for publication in a future issue of this journal, but has not been fully edited. Content may change prior to final publication. Citation information: DOI10.1109/tvt.2023.3265963, IEEE Transactions on Vehicular Technology

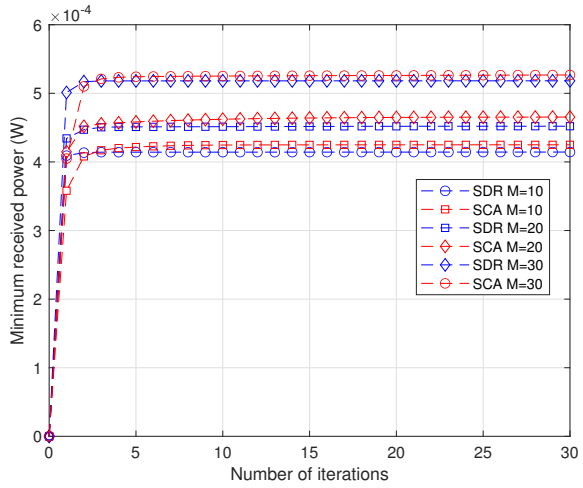

Fig. 3. Convergence of the proposed SDR-based AO algorithm and SCA-based AO algorithms for different values of M.

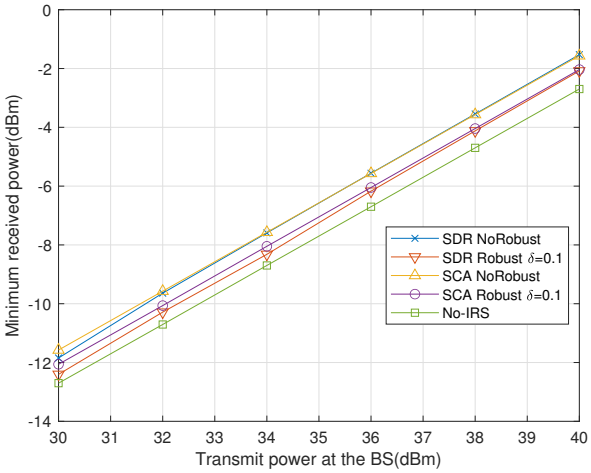

Fig. 5. The minimum received power versus the transmit power at the BS.

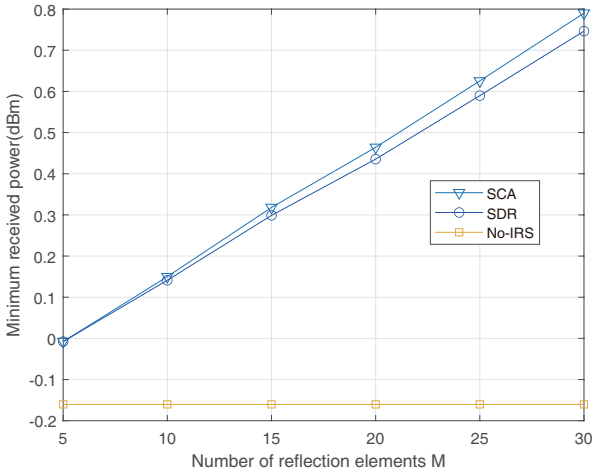

Fig. 4. The minimum received power versus the number of IRS elements.

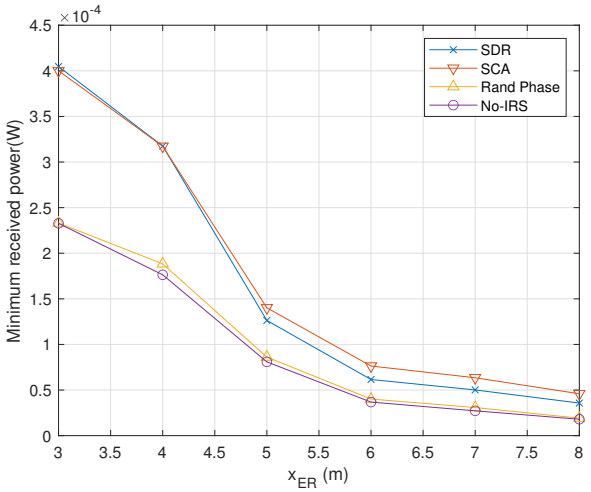

Fig. 6. The minimum received power versus x_{ER}.

C. Minimum Received Power Versus Number of Reflecting Elements

In Fig. 4, we compare the ER's minimum received power of various algorithms versus the number of reflecting elements M. The minimum received power at ER achieved by two algorithms increases with M, since the IRS can create additional links and improve the channel environment by properly adjusting the phase shifts. By deploying the IRS in the SWIPT system, the received power at ER obtained by our proposed two algorithms becomes higher than the scheme which does not consider IRS. Additionally, we can observe that the SCA-based AO algorithm is better than the SDR-based AO algorithm, and the gap becomes large with the increase of M. This can be explained as follows. When the number of the reflecting elements M is small, the rank-one feasible solution region is large. As a result, for a given number of random times, the Gaussian randomization method may find the optimal solution. However, when M is too large, the rank-one feasible solution region is small, so in given number of random times, the Gaussian randomization method can only achieve a sub-optimal solution.

D. Minimum Received Power Versus Transmit Power

In Fig. 5, we investigate the impact of transmit power at the BS on the EH performance of ERs. The minimum received power achieved by all schemes monotonically increases with the increase of the transmit power at the BS. Additionally, we observe that the minimum received power of the robust beamforming design scheme is lower than no-robust beamforming scheme. This is because the robust beamforming design considers the worst channel condition and it is the price to pay for the robust design. Finally, we also find that the transmit power at the BS has a great impact on the received power.

E. Minimum Received Power Versus The Distance From BS To Energy Receivers

In Fig. 6, we investigate the impact of the distance between BS and ERs on the received power. We can see the received power decreases gradually with the increase of distance from

This article has been accepted for publication in a future issue of this journal, but has not been fully edited. Content may change prior to final publication. Citation information: DOI10.1109/tvt.2023.3265963, IEEE Transactions on Vehicular Technology

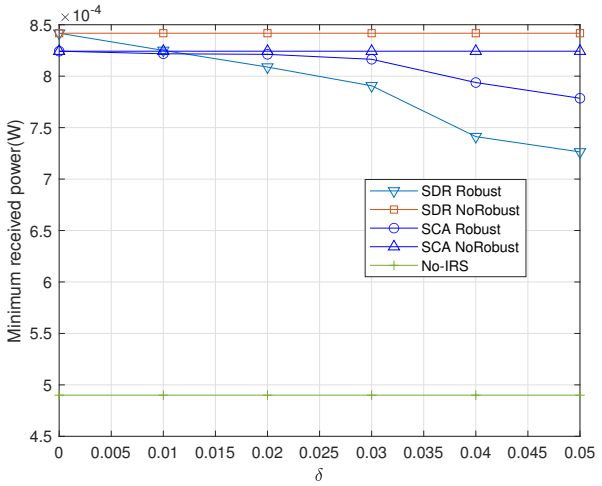

Fig. 7. The minimum received power versus channel estimate error coefficient δ.

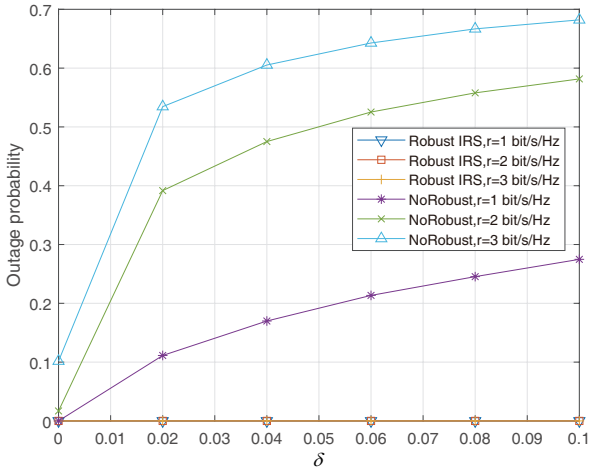

Fig. 8. Outage probability of rate versus channel estimate error coefficient δ.

the BS to the ERs. This is because when the distance increases, the path loss increases, and causes the decrease of the received power. We also find that the received power of ERs is greatly affected by the distance from the BS to ERs, which shows that the ERs should be placed close to the BS. Additionally, we note that deploying IRS can increase the received power compared to no IRS. Finally, it can be seen from Fig. 6 that compared with random phase, where the phase shift matrix of the IRS has not been optimized, the received power is improved after we optimize the phase shift matrix. This illustrates the importance of optimizing the phase shift matrix of the IRS.

F. Minimum Received Power Versus Channel Estimate Error

In Fig. 7, the impact of channel estimation error coefficient δ is studied. Note that the received power gleaned by robust beamforming schemes decreases with the increase of the channel estimate error. This is expected since more beams need to be directed towards the information receiver to ensure the minimum rate requirements of the IRs and the robustness of the system. Therefore, the receiving power of the energy receivers are reduced. It is also observed from Fig. 7 that the received power of robust beamforming design scheme is lower than that of no-robust, this is because the robust beamforming scheme considers the worst channel case, and thus leading to lower received power than no-robust. However, it is still higher than the 'No IRS' setup. In addition, we note that the performance of the SDR-based algorithm is better than that of the SCA-based algorithm when the channel estimation error coefficient δ is small, however, this result is just the opposite when δ is large. This typical value is 0.01. This enlightens us that we can choose the best algorithm according to the channel estimation error value.

G. Outage Probability of Rate Versus Channel Estimate Error

In Fig. 8, we investigate the impact of channel estimation error coefficient δ on the outage probability of the rate. Specifically, we define the probability that the IR rate is lower than the minimum rate as the outage probability. It is observed that no-robust scheme often has outage, and the outage probability monotonically increases with the increase of the channel estimate error coefficient δ and minimum rate requirement. Our proposed robust beamforming design algorithm can guarantee to have zero probability of outage.

V. Conclusion

In this paper, we have studied robust beamforming designs under imperfect cascaded channel for the IRS-aided MISO SWIPT system. In order to ensure fairness, our aim was to maximize the minimum received energy among all ERs, subject to the worst-case rate constraints. Two novel algorithms, which use SCA or SDR methods are proposed to jointly optimize the active beamforming vectors at the BS and passive phase shift matrix at the IRS, respectively. Specially, the CSI uncertainties were addressed by using transformation techniques and S-procedure, the SCA, penalty CCP and SDR methods were used to deal with the non-convex constraints. Numerical results demonstrated that deploy IRS in SWIPT system can enhance the harvested power of ERs. Our proposed algorithms can guarantee system robustness with rapid convergence.

Appendix A
Proof of the Lemma 1

According to Lemma 3 in [31], the linear approximation of $|\boldsymbol{g}_{d,j}^H + \boldsymbol{e}^H(\bar{\boldsymbol{G}}_j + \Delta\boldsymbol{G}_j)\boldsymbol{w}_i|^2$ at $(\boldsymbol{w}_i^{(n)}, \boldsymbol{e}^{(n)})$ can be expressed as

$$\mathrm{vec}^{\mathrm{T}}(\Delta\mathbf{G}_j)\mathbf{B}_i\,\mathrm{vec}(\Delta\mathbf{G}_j^*) + 2\,\mathrm{Re}\{\mathbf{b}_i^{\mathrm{T}}\,\mathrm{vec}(\Delta\mathbf{G}_j^*)\} + d_i, \quad (47)$$

This article has been accepted for publication in a future issue of this journal, but has not been fully edited. Content may change prior to final publication. Citation information: DOI10.1109/tvt.2023.3265963, IEEE Transactions on Vehicular Technology

where

$$\begin{aligned}\mathbf{B}_i =&\boldsymbol{w}_i\boldsymbol{w}_i^{(n),H}\otimes\boldsymbol{e}^*\boldsymbol{e}^{(n),T}+\boldsymbol{w}_i^{(n)}\boldsymbol{w}_i^H\otimes\boldsymbol{e}^{(n),*}\boldsymbol{e}^T\\&-\boldsymbol{w}_i^{(n)}\boldsymbol{w}_i^{(n),H}\otimes\boldsymbol{e}^{(n),*}\boldsymbol{e}^{(n),T},\\\mathbf{b}_i =&\operatorname{vec}(\boldsymbol{e}(\boldsymbol{g}_{d,j}^H+\boldsymbol{e}^{(n),H}\bar{\boldsymbol{G}}_j)\boldsymbol{w}_i^{(n)}\boldsymbol{w}_i^H)\\&+\operatorname{vec}(\boldsymbol{e}^{(n)}(\boldsymbol{g}_{d,j}^H+\boldsymbol{e}^H\bar{\boldsymbol{G}}_j)\boldsymbol{w}_i\boldsymbol{w}_i^{(n),H})\\&-\operatorname{vec}(\boldsymbol{e}^{(n)}(\boldsymbol{g}_{d,j}^H+\boldsymbol{e}^{(n),H}\bar{\boldsymbol{G}}_j)\boldsymbol{w}_i^{(n)}\boldsymbol{w}_i^{(n),H}),\\d_i =&2\operatorname{Re}\{(\boldsymbol{g}_{d,j}^H+\boldsymbol{e}^{(n),H}\bar{\boldsymbol{G}}_j)\boldsymbol{w}_i^{(n)}\boldsymbol{w}_i^H(\boldsymbol{g}_{d,j}+\bar{\boldsymbol{G}}_j^H\boldsymbol{e})\}\\&-(\boldsymbol{g}_{d,j}^H+\boldsymbol{e}^{(n),H}\bar{\boldsymbol{G}}_j)\boldsymbol{w}_i^{(n)}\boldsymbol{w}_i^{(n),H}(\boldsymbol{g}_{d,j}+\bar{\boldsymbol{G}}_j^H\boldsymbol{e}^{(n)}).\end{aligned}$$

Then, according to the addition rule for derivatives, the linear approximation of $\sum_{i\in\mathcal{K}_I}|(\boldsymbol{g}_{d,j}^H+\boldsymbol{e}^H\boldsymbol{G}_j)\boldsymbol{w}_i)|^2+\sum_{k\in\mathcal{K}_E}|(\boldsymbol{g}_{d,j}^H+\boldsymbol{e}^H\boldsymbol{G}_j)\boldsymbol{v}_k|^2$ at $(\boldsymbol{w}_1^{(n)},...,\boldsymbol{w}_{K_I}^{(n)},\boldsymbol{v}_1^{(n)},...,\boldsymbol{v}_{K_E}^{(n)},\boldsymbol{e}^n)$ can be expressed as

$$\begin{aligned}&\sum(\operatorname{vec}^{\mathrm{T}}(\Delta\mathbf{G}_j)\mathbf{B}_i\operatorname{vec}(\Delta\mathbf{G}_j^*)+2\operatorname{Re}\{\mathbf{b}_i^{\mathrm{T}}\operatorname{vec}(\Delta\mathbf{G}_j^*)\}+d_i)\\&=\operatorname{vec}^{\mathrm{T}}(\Delta\mathbf{G}_j)(\sum\mathbf{B}_i)\operatorname{vec}(\Delta\mathbf{G}_j^*)\\&\quad+2\operatorname{Re}\{(\sum\mathbf{b}_i)^{\mathrm{T}}\operatorname{vec}(\Delta\mathbf{G}_j^*)\}+\sum d_i.\end{aligned}$$

By defining

$$\begin{aligned}\mathbf{A}_j=&\sum\mathbf{B}_i\\=&(\sum_{i\in\mathcal{K}_I}\boldsymbol{w}_i\boldsymbol{w}_i^{(n),H}+\sum_{j\in\mathcal{K}_E}\boldsymbol{v}_j\boldsymbol{v}_j^{(n),H})\otimes\boldsymbol{e}^*\boldsymbol{e}^{(n),T}\\&+(\sum_{i\in\mathcal{K}_I}\boldsymbol{w}_i^{(n)}\boldsymbol{w}_i^H+\sum_{j\in\mathcal{K}_E}\boldsymbol{v}_j^{(n)}\boldsymbol{v}_j^H)\otimes\boldsymbol{e}^{(n),*}\boldsymbol{e}^T\\&-(\sum_{i\in\mathcal{K}_I}\boldsymbol{w}_i^{(n)}\boldsymbol{w}_i^{(n),H}+\sum_{j\in\mathcal{K}_E}\boldsymbol{v}_j^{(n)}\boldsymbol{v}_j^{(n),H})\otimes\boldsymbol{e}^{(n),*}\boldsymbol{e}^{(n),T},\\\boldsymbol{c}=&\sum_{i\in\mathcal{K}_I}\boldsymbol{w}_i\boldsymbol{w}_i^{(n),H}+\sum_{j\in\mathcal{K}_E}\boldsymbol{v}_j\boldsymbol{v}_j^{(n),H},\end{aligned}$$

we can obtained (12), the proof is completed.

Appendix B
Proof of the lemma 4

By relaxing the rank-one constraint in Problem (P8.1), the remaining problem is an SDP problem, which is convex. This problem satisfies the Slater's constraint qualification. There is a zero duality gap, and thus strong duality holds. The Lagrangian function expressed as

$$\begin{aligned}\mathcal{L}=&-\sum_{i\in\mathcal{K}_I}[\operatorname{Tr}(\mathbf{Y}_i\mathbf{W}_i)\\&-\operatorname{Tr}\left(\mathbf{B}_i\mathbf{P}_i^H\left(\boldsymbol{\Phi}^T\otimes\bar{\mathbf{W}}_i\right)\mathbf{P}_i\right)-\beta\operatorname{Tr}(\mathbf{W}_i)]\\&-\sum_{j\in\mathcal{K}_E}[\operatorname{Tr}(\mathbf{A}_j\mathbf{V}_j)-\operatorname{Tr}\left(\mathbf{D}_j\mathbf{Z}_j^H\left(\boldsymbol{\Phi}^T\otimes\mathbf{C}\right)\mathbf{Z}_j\right)\\&-\beta\operatorname{Tr}(\mathbf{V}_j)]+c,\end{aligned}\tag{48}$$

where $\mathbf{Y}_i,\mathbf{A}_j$ are the dual variables associated with constraints $\mathbf{W}_i\succeq\mathbf{0}$ and $\mathbf{V}_j\succeq\mathbf{0}$, respectively. $\mathbf{B}_i$ and $\mathbf{D}_j$ are the dual variables associated with (36) and (39), respectively. c represents the collection of terms that do not depend on $\mathbf{W}_i$ and $\mathbf{V}_j$. Then, the complementary slackness conditions for problem (P8.1) without rank-one constraint are given by

$$\begin{aligned}&\mathrm{K1}:\mathbf{Y}_i^{\mathrm{opt}}\succeq\mathbf{0},\mathbf{B}_i^{\mathrm{opt}}\succeq\mathbf{0},\mathbf{A}_j^{\mathrm{opt}}\succeq\mathbf{0},\mathbf{D}_j^{\mathrm{opt}}\succeq\mathbf{0},\\&\mathrm{K2}:\mathbf{Y}_i^{\mathrm{opt}}\mathbf{W}_i^{\mathrm{opt}}=\mathbf{0},\mathbf{A}_j^{\mathrm{opt}}\mathbf{V}_j^{\mathrm{opt}}=\mathbf{0},\\&\mathrm{K3}:\nabla_{\mathbf{W}_i}\mathcal{L}\left(\mathbf{W}_i^{\mathrm{opt}}\right)=\mathbf{0},\\&\mathrm{K4}:\nabla_{\mathbf{V}_j}\mathcal{L}\left(\mathbf{V}_j^{\mathrm{opt}}\right)=\mathbf{0},\forall i\in\mathcal{K}_I,j\in\mathcal{K}_E.\end{aligned}\tag{49}$$

Firstly, we prove $\operatorname{Rank}(\mathbf{W}_i)=1$. Noted that complementary slackness conditions K3 can be rewritten as

$$\mathbf{Y}_i^{\mathrm{opt}}=\beta\mathbf{I}_N-\boldsymbol{\Upsilon}_i^{\mathrm{opt}},\tag{50}$$

where $\boldsymbol{\Upsilon}_i^{\mathrm{opt}}=\mathbf{T}_i^{\mathrm{opt}}-\sum_{k\in\mathcal{K}_I\setminus\{i\}}\gamma_i\mathbf{T}_i^{\mathrm{opt}}$, and the matrix $\mathbf{T}_i^{\mathrm{opt}}$ is given by

$$\mathbf{T}_i^{\mathrm{opt}}=\sum_{i=1}^{M+1}\sum_{j=1}^{M+1}a_{ij}\mathbf{U}_{ij}^{\mathrm{opt}},\tag{51}$$

where a_{ij} is the (i,j)-th element of $\boldsymbol{\Phi}$ and $\mathbf{U}_{ij}^{\mathrm{opt}}\in\mathbb{C}^{N\times N}$ is the (i,j)-th submatrix of $\mathbf{P}_i\mathbf{B}_i^{\mathrm{opt}}\mathbf{P}_i^H$,

$$\mathbf{P}_i\mathbf{B}_i^{\mathrm{opt}}\mathbf{P}_i^H=\begin{bmatrix}\mathbf{U}_{11}^{\mathrm{opt}}&\mathbf{U}_{12}^{\mathrm{opt}}&\cdots&\mathbf{U}_{1(M+1)}^{\mathrm{opt}}\\\mathbf{U}_{21}^{\mathrm{opt}}&&&\\\vdots&&\ddots&\\\mathbf{U}_{(M+1)1}^{\mathrm{opt}}&&&\mathbf{U}_{(M+1)(M+1)}^{\mathrm{opt}}\end{bmatrix}.\tag{52}$$

Due to user channels are distributed independently, the probability of having multiple identical eigenvalues $\lambda_{\max}\left(\boldsymbol{\Upsilon}_i^{\mathrm{opt}}\right)$ is zero. For (50), if $\lambda_{\max}\left(\boldsymbol{\Upsilon}_i^{\mathrm{opt}}\right)>\beta$, then $\mathbf{Y}_i^{\mathrm{opt}}\succeq\mathbf{0}$ does not hold, which contradicts to K1. Additionally, if $\lambda_{\max}\left(\boldsymbol{\Upsilon}_i^{\mathrm{opt}}\right)\leq\beta$, then $\mathbf{Y}_i^{\mathrm{opt}}$ is a positive semidefinite matrix with $\operatorname{Rank}(\mathbf{Y}_i^{\mathrm{opt}})\geq N-1$, which leads to $\operatorname{Rank}(\mathbf{W}_i^{\mathrm{opt}})\leq1$ because of K2. In addition, due to the SINR constraints, it must hold that $\mathbf{W}_i^{\mathrm{opt}}\neq\mathbf{0}$. Therefore, $\operatorname{Rank}(\mathbf{W}_i^{\mathrm{opt}})=1$. By applying similar analysis, $\operatorname{Rank}(\mathbf{V}_j^{\mathrm{opt}})\leq1$ can be obtained, the proof is completed.

References

[1] J. Xu, L. Liu, and R. Zhang, "Multiuser MISO beamforming for simultaneous wireless information and power transfer," *IEEE Trans. Signal Process.*, vol. 62, no. 18, pp. 4798–4810, 2014.

[2] R. Zhang and C. K. Ho, "MIMO broadcasting for simultaneous wireless information and power transfer," *IEEE Trans. Wireless Commun.*, vol. 12, no. 5, pp. 1989–2001, 2013.

[3] X. Lu, P. Wang, D. Niyato, D. I. Kim, and Z. Han, "Wireless networks with rf energy harvesting: A contemporary survey," *IEEE Commun. Surv. Tuts.*, vol. 17, no. 2, pp. 757–789, 2015.

[4] W. Feng, J. Tang, Y. Yu, J. Song, N. Zhao, G. Chen, K.-K. Wong, and J. Chambers, "UAV-enabled SWIPT in IoT networks for emergency communications," *IEEE Wireless Commun.*, vol. 27, no. 5, pp. 140–147, 2020.

[5] L. Liu, R. Zhang, and K.-C. Chua, "Secrecy wireless information and power transfer with MISO beamforming," *IEEE Trans. Signal Process.*, vol. 62, no. 7, pp. 1850–1863, 2014.

[6] D. W. K. Ng, E. S. Lo, and R. Schober, "Robust beamforming for secure communication in systems with wireless information and power transfer," *IEEE Trans. Wireless Commun.*, vol. 13, no. 8, pp. 4599–4615, 2014.

[7] L. Lu, G. Y. Li, A. L. Swindlehurst, A. Ashikhmin, and R. Zhang, "An overview of massive MIMO: Benefits and challenges," *IEEE J. Sel. Topics Signal Process.*, vol. 8, no. 5, pp. 742–758, 2014.

[8] C. Pan, H. Ren, K. Wang, J. F. Kolb, M. Elkashlan, M. Chen, M. Di Renzo, Y. Hao, J. Wang, A. L. Swindlehurst, X. You, and L. Hanzo, "Reconfigurable intelligent surfaces for 6G systems: Principles, applications, and research directions," *IEEE Commun. Mag.*, vol. 59, no. 6, pp. 14–20, 2021.

[9] Q. Wu and R. Zhang, "Intelligent reflecting surface enhanced wireless network via joint active and passive beamforming," *IEEE Trans. Wireless Commun.*, vol. 18, no. 11, pp. 5394–5409, 2019.

[10] S. Zhang and R. Zhang, "Capacity characterization for intelligent reflecting surface aided MIMO communication," *IEEE J. Sel. Areas Commun.*, vol. 38, no. 8, pp. 1823–1838, 2020.

[11] C. Huang, A. Zappone, G. C. Alexandropoulos, M. Debbah, and C. Yuen, "Reconfigurable intelligent surfaces for energy efficiency in wireless communication," *IEEE Trans. Wireless Commun.*, vol. 18, no. 8, pp. 4157–4170, 2019.

[12] C. Zhang, W. Chen, C. He, and X. Li, "Throughput maximization for intelligent reflecting surface-aided device-to-device communications system," *J. Commun. Inf. Netw.*, vol. 5, no. 4, pp. 403–410, 2020.

[13] H. Xie, J. Xu, and Y.-F. Liu, "Max-min fairness in IRS-aided multi-cell MISO systems with joint transmit and reflective beamforming," *IEEE Trans. Wireless Commun.*, vol. 20, no. 2, pp. 1379–1393, 2021.

[14] J. Zhao, Q. Li, Y. Gong, and K. Zhang, "Computation offloading and resource allocation for cloud assisted mobile edge computing in vehicular networks," *IEEE Trans. Veh. Technol.*, vol. 68, no. 8, pp. 7944–7956, 2019.

[15] T. Bai, C. Pan, Y. Deng, M. Elkashlan, A. Nallanathan, and L. Hanzo, "Latency minimization for intelligent reflecting surface aided mobile edge computing," *IEEE J. Sel. Areas Commun.*, vol. 38, no. 11, pp. 2666–2682, 2020.

[16] X. Yu, D. Xu, Y. Sun, D. W. K. Ng, and R. Schober, "Robust and secure wireless communications via intelligent reflecting surfaces," *IEEE J. Sel. Areas Commun.*, vol. 38, no. 11, pp. 2637–2652, 2020.

[17] S. Hong, C. Pan, H. Ren, K. Wang, and A. Nallanathan, "Artificial-noise-aided secure MIMO wireless communications via intelligent reflecting surface," *IEEE Trans. Commun.*, vol. 68, no. 12, pp. 7851–7866, 2020.

[18] H. Shen, W. Xu, S. Gong, Z. He, and C. Zhao, "Secrecy rate maximization for intelligent reflecting surface assisted multi-antenna communications," *IEEE Commun. Lett.*, vol. 23, no. 9, pp. 1488–1492, 2019.

[19] S. Fang, G. Chen, and Y. Li, "Joint optimization for secure intelligent reflecting surface assisted UAV networks," *IEEE Wireless Commun. Lett.*, vol. 10, no. 2, pp. 276–280, 2021.

[20] C. Pan, H. Ren, K. Wang, M. Elkashlan, A. Nallanathan, J. Wang, and L. Hanzo, "Intelligent reflecting surface aided MIMO broadcasting for simultaneous wireless information and power transfer," *IEEE J. Sel. Areas Commun.*, vol. 38, no. 8, pp. 1719–1734, 2020.

[21] Q. Wu and R. Zhang, "Joint active and passive beamforming optimization for intelligent reflecting surface assisted SWIPT under QoS constraints," *IEEE J. Sel. Areas Commun.*, vol. 38, no. 8, pp. 1735–1748, 2020.

[22] S. Zargari, A. Khalili, and R. Zhang, "Energy efficiency maximization via joint active and passive beamforming design for multiuser MISO IRS-aided SWIPT," *IEEE Wireless Commun. Lett.*, vol. 10, no. 3, pp. 557–561, 2021.

[23] Q. Wu and R. Zhang, "Weighted sum power maximization for intelligent reflecting surface aided SWIPT," *IEEE Wireless Commun. Lett.*, vol. 9, no. 5, pp. 586–590, 2020.

[24] Y. Tang, G. Ma, H. Xie, J. Xu, and X. Han, "Joint transmit and reflective beamforming design for IRS-assisted multiuser MISO SWIPT systems," in *Proc. IEEE Int. Conf. Commun.*, 2020, pp. 1–6.

[25] H. Zhang and B. Di, "Intelligent omni-surfaces: Simultaneous refraction and reflection for full-dimensional wireless communications," *IEEE Commun. Surv. Tuts.*, vol. 24, no. 4, pp. 1997–2028, 2022.

[26] M. H. Khoshafa, T. M. N. Ngatched, M. H. Ahmed, and A. R. Ndjiongue, "Active reconfigurable intelligent surfaces-aided wireless communication system," *IEEE Commun. Lett.*, vol. 25, no. 11, pp. 3699–3703, 2021.

[27] Y. Gao, Q. Wu, G. Zhang, W. Chen, D. W. K. Ng, and M. D. Renzo, "Beamforming optimization for active intelligent reflecting surface-aided SWIPT," *IEEE Trans. Wireless Commun.*, vol. 22, no. 1, pp. 362–378, 2023.

[28] P. Zeng, D. Qiao, Q. Wu, and Y. Wu, "Throughput maximization for active intelligent reflecting surface-aided wireless powered communications," *IEEE Wireless Commun. Lett.*, vol. 11, no. 5, pp. 992–996, 2022.

[29] C. You and R. Zhang, "Wireless communication aided by intelligent reflecting surface: Active or passive?" *IEEE Wireless Commun. Lett.*, vol. 10, no. 12, pp. 2659–2663, 2021.

[30] G. Zhou, C. Pan, H. Ren, K. Wang, M. D. Renzo, and A. Nallanathan, "Robust beamforming design for intelligent reflecting surface aided MISO communication systems," *IEEE Wireless Commun. Lett.*, vol. 9, no. 10, pp. 1658–1662, 2020.

[31] G. Zhou, C. Pan, H. Ren, K. Wang, and A. Nallanathan, "A framework of robust transmission design for IRS-aided MISO communications with imperfect cascaded channels," *IEEE Trans. Signal Process.*, vol. 68, pp. 5092–5106, 2020.

[32] X. Yu, D. Xu, D. W. K. Ng, and R. Schober, "IRS-assisted green communication systems: Provable convergence and robust optimization," *IEEE Trans. Commun.*, vol. 69, no. 9, pp. 6313–6329, 2021.

[33] S. Zargari, S. Farahmand, B. Abolhassani, and C. Tellambura, "Robust active and passive beamformer design for IRS-aided downlink MISO PS-SWIPT with a nonlinear energy harvesting model," *IEEE Trans. Green Commun. Netw.*, vol. 5, no. 4, pp. 2027–2041, 2021.

[34] H. Niu, Z. Chu, F. Zhou, Z. Zhu, L. Zhen, and K.-K. Wong, "Robust design for intelligent reflecting surface assisted secrecy SWIPT network," *IEEE Trans. Wireless Commun.*, pp. 1–1, 2021.

[35] D. Mishra, G. C. Alexandropoulos, and S. De, "Energy sustainable IoT with individual QoS constraints through MISO SWIPT multicasting," *IEEE Internet Things J.*, vol. 5, no. 4, pp. 2856–2867, 2018.

[36] Y. Liu, H. Zhang, B. Di, J. Wu, and Z. Han, "Deployment for high altitude platform systems with perturbation: Distributionally robust optimization approach," *IEEE Commun. Lett.*, vol. 26, no. 5, pp. 1126–1130, 2022.

[37] X. Li, C. Zhang, C. He, G. Chen, and J. A. Chambers, "Sum-rate maximization in IRS-assisted wireless power communication networks," *IEEE Internet Things J.*, vol. 8, no. 19, pp. 14 959–14 970, 2021.

[38] W. Zhang, J. Xu, W. Xu, D. W. K. Ng, and H. Sun, "Cascaded channel estimation for IRS-assisted mmWave multi-antenna with quantized beamforming," *IEEE Commun. Lett.*, vol. 25, no. 2, pp. 593–597, 2021.

[39] Z. Wang, L. Liu, and S. Cui, "Channel estimation for intelligent reflecting surface assisted multiuser communications: Framework, algorithms, and analysis," *IEEE Trans. Wireless Commun.*, vol. 19, no. 10, pp. 6607–6620, 2020.

[40] Y. Lu, K. Xiong, P. Fan, Z. Zhong, B. Ai, and K. B. Letaief, "Worst-case energy efficiency in secure SWIPT networks with rate-splitting ID and power-splitting EH receivers," *IEEE Trans. Wireless Commun.*, pp. 1–1, 2021.

[41] S. Boyd, S. P. Boyd, and L. Vandenberghe, *Convex optimization*. Cambridge university press, 2004.

[42] A. Garces, *Convex optimization*, 2022, pp. 39–59.

[43] E. A. Gharavol and E. G. Larsson, "The sign-definiteness lemma and its applications to robust transceiver optimization for multiuser MIMO systems," *IEEE Trans. Signal Process.*, vol. 61, no. 2, pp. 238–252, 2013.

[44] K.-Y. Wang, A. M.-C. So, T.-H. Chang, W.-K. Ma, and C.-Y. Chi, "Outage constrained robust transmit optimization for multiuser MISO downlinks: Tractable approximations by conic optimization," *IEEE Trans. Signal Process.*, vol. 62, no. 21, pp. 5690–5705, 2014.

Chiya Zhang received the Ph.D. degree in Telecommunication Engineering from the University of New South Wales, Sydney, Australia, in 2019. He is currently an Associate Professor at Harbin Institute of Technology, Shenzhen, China. His current research interest is AI applications in telecommunication engineering. He received the Exemplary Reviewer Certificates of the IEEE Wireless Communications Letters in 2018 and IEEE ComSoc Asia-Pacific Outstanding Paper Award in 2020. He is serving as an Associate Editor for the IEEE Internet of Things Journal.

Yin Huang received his B.S. degree in electronic information engineering from Henan Polytechnic University, Henan, China, in 2019. He is a master student of communication engineering with the Guangdong Key Laboratory of Intelligent Information Processing, College of Electronics and Information Engineering, Shenzhen University, Shenzhen, China. His research interests include intelligent reflecting surface and SWIPT communications.

Chunlong He received the M.S. degree in Communication and Information Science from Southwest Jiaotong University, Chengdu, China, in 2010 and the Ph.D. degree from Southeast University, Nanjing, China, in 2014. From September 2012 to September 2014, he was a Visiting Student with the School of Electrical and Computer Engineering, Georgia Institute of Technology, Atlanta, GA, USA. Since 2015, he has been with the College of Information Engineering, Shenzhen University, where he is currently an Associate Professor. His research interests include communication and signal processing, green communication systems, channel estimation algorithms, and limited feedback techniques. Dr. He is a member of the Institute of Electronics, Information, and Communication Engineering. He is currently an Associate Editor of IEEE Access.

Cunhua Pan received the B.S. and Ph.D. degrees from the School of Information Science and Engineering, Southeast University, Nanjing, China, in 2010 and 2015, respectively. From 2015 to 2016, he was a Research Associate at the University of Kent, U.K. He held a post-doctoral position at Queen Mary University of London, U.K., from 2016 and 2019, where he is currently a Professor at Southeast University, Nanjing, China. His research interests mainly include ultra-dense C-RAN, machine learning, UAV, Internet of Things, and mobile edge computing. He serves as a TPC member for numerous conferences, such as ICC and GLOBECOM, and the Student Travel Grant Chair for ICC 2019. He also serves as an Editor of IEEE Wireless Communication Letters and IEEE ACCESS.

Kezhi Wang received the B.E. and the M.E. degrees in School of Automation from Chongqing University, Chongqing, China, in 2008 and 2011, respectively. He received the Ph.D. degree in Engineering from the University of Warwick, Coventry, U.K. in 2015. He was a Senior Research Officer in University of Essex, Essex, U.K. Currently, he is an Assistant Professor with Department of Computer Science, Brunel University London, Uxbridge, Middlesex, UK. His research interests include wireless communications and machine learning.